NeuroMolecular Medicine (2019) 21:414–431
https://doi.org/10.1007/s12017-019-08531-z

ORIGINAL PAPER

Oxygen-Glucose Deprivation/Reoxygenation-Induced Barrier Disruption at the Human Blood–Brain Barrier is Partially Mediated Through the HIF-1 Pathway

Shyanne Page[1] · Snehal Raut[1] · Abraham Al-Ahmad[1]

Received: 12 November 2018 / Accepted: 12 March 2019 / Published online: 26 March 2019

Abstract

The blood–brain barrier (BBB) plays an important role in brain homeostasis. Hypoxia/ischemia constitutes an important stress factor involved in several neurological disorders by inducing the disruption of the BBB, ultimately leading to cerebral edema formation. Yet, our current understanding of the cellular and molecular mechanisms underlying the BBB disruption following cerebral hypoxia/ischemia remains limited. Stem cell-based models of the human BBB present some potentials to address such issues. Yet, such models have not been validated in regard of its ability to respond to hypoxia/ischemia as existing models. In this study, we investigated the cellular response of two iPSC-derived brain microvascular endothelial cell (BMEC) monolayers to respond to oxygen-glucose deprivation (OGD) stress, using two induced pluripotent stem cells (iPSC) lines. iPSC-derived BMECs responded to prolonged (24 h) and acute (6 h) OGD by showing a decrease in the barrier function and a decrease in tight junction complexes. Such iPSC-derived BMECs responded to OGD stress via a partial activation of the HIF-1 pathway, whereas treatment with anti-angiogenic pharmacological inhibitors (sorafenib, sunitinib) during reoxygenation worsened the barrier function. Taken together, our results suggest such models can respond to hypoxia/ischemia similarly to existing in vitro models and support the possible use of this model as a screening platform for identifying novel drug candidates capable to restore the barrier function following hypoxic/ischemic injury.

Keywords Blood–brain barrier · Stem cells · Cerebral ischemia · Hypoxia · Reoxygenation

Introduction

The blood–brain barrier (BBB) plays an important role in brain homeostasis, by providing a physical and chemical barrier against toxicants and pathogens (Neuwelt et al. 2011). Disruption of the BBB is a hallmark feature associated with the pathophysiology of several neurological disorders including adrenoleukodystrophy (Orchard et al. 2019; Lee et al. 2018), Alzheimer's disease (Nation et al. 2019; Sweeney et al. 2019), Huntington's disease (Lim et al. 2017; Drouin-Ouellet et al. 2015), stroke (Merali et al. 2017; Turner and Sharp 2016; Choi et al. 2016; Suzuki et al. 2016; Kassner and Merali 2015; Prakash and Carmichael 2015), or traumatic brain injury (Wu et al. 2017; Wang et al. 2016a, b; Prakash and Carmichael 2015; Dore-Duffy et al. 2000).

Hypoxia/ischemia is an important environmental stress factor involved in several diseases associated with a disruption of the BBB such as cerebral ischemia (Kim et al. 2018a, b; Lu et al. 2018; Haley and Lawrence 2017; Merali et al. 2017; Turner and Sharp 2016; Choi et al. 2016; Suzuki et al. 2016; Kassner and Merali 2015; Prakash and Carmichael 2015; O'Donnell 2014; Kuntz et al. 2014; Yang et al. 2013; Fernandez-Lopez et al. 2012), cerebral amyloid angiopathy (Freeze et al. 2019; Daulatzai 2017; Ghiso et al. 2014), high-altitude cerebral edema (Lafuente et al. 2016; Ogunshola and Al-Ahmad 2012; Natah et al. 2009; Hackett and Roach 2004; Mark and Davis 2002; Schoch et al. 2002), or neonatal hypoxic/ischemic encephalitis (Lee et al. 2017; Ma et al. 2017; Gussenhoven et al. 2019). Disruption of the BBB following hypoxic/ischemic event has been

Electronic supplementary material The online version of this article (https://doi.org/10.1007/s12017-019-08531-z) contains supplementary material, which is available to authorized users.

✉ Abraham Al-Ahmad
abraham.al-ahmad@ttuhsc.edu

[1] Department of Pharmaceutical Sciences, School of Pharmacy, Texas Tech University Health Sciences Center, 1300 South Coulter Street, Amarillo, TX 79106, USA

documented with a loss of tight junction complexes (Kokubu et al. 2017; Zhang et al. 2016; Page et al. 2016; Engelhardt et al. 2015, 2014a, 2014b; Al Ahmad et al. 2012; Ogunshola and Al-Ahmad 2012; Zhu et al. 2012; Al Ahmad et al. 2011; Bauer et al. 2010; Haarmann et al. 2010; Al Ahmad et al. 2009), resulting in cerebral edema formation, a potentially fatal condition. At the BBB, brain microvascular endothelial cells (BMECs) constitute the first cell type of the neurovascular unit to respond to hypoxic/ischemic injury, via the activation of the hypoxia-inducible factor (HIF) pathway (Ogunshola and Al-Ahmad 2012). Under hypoxia/ischemia, HIF-1α undergoes a rapid stabilization, resulting in its nuclear translocation, pairing with HIF-1β/aryl hydrocarbon receptor nuclear translocase (ARNT) to form the HIF-1 transcription factor complex. HIF-1 has been documented to modulate the expression of over 200 target genes including vascular endothelial growth factor (VEGF) and matrix metalloproteinases (MMP-2, MMP-9), two class of proteins well documented for their contribution of the BBB disruption (Zhang et al. 2018; Turner and Sharp 2016; Jin et al. 2015; Yang et al. 2013; Liu et al. 2012, 2009; Feng et al. 2011; Bauer et al. 2010). The current literature investigating the effect of cerebral hypoxia/ischemia in vitro and in vivo is predominantly documented from rodent-based models. Yet, in vitro models of the BBB used in such studies suffer from the presence of poor barrier properties (Helms et al. 2016; Holloway and Gavins 2016; Palmiotti et al. 2014; Naik and Cucullo 2012; Ogunshola 2011), making their relevance to understand the cellular and molecular mechanisms underlying the disruption of the BBB limited. More recently, human in vitro models of the BBB based on stem cells have been documented. Such models provide a scalable source of cells, BMECs displayed a phenotype and gene expression profile close from primary human BMECs and were capable to form significantly tighter monolayers. However, the ability of these monolayers to respond to hypoxia/ischemia as previous in vitro models remains poorly documented (Page et al. 2016; Kokubu et al. 2017). The major aim of this study is to investigate the cellular response of stem cell derived in vitro models of the BBB, using two patient-derived induced pluripotent stem cells (iPSCs).

Materials and Methods

Cell Culture

The hCMEC/D3 immortalized human brain microvascular cell line (RRID: CVCL_U985) was purchased from EMD Millipore (Billerica, MA, USA) and maintained following the manufacturer's instructions. This cell line was originally isolated from a female patient suffering from temporal lobe epilepsy (Weksler et al. 2005). CTR90F (Yu et al. 2007) (IPS(IMR90)-c4; RRID: CVCL_C437) and CTR65M (ND41865, RRID: CVCL_Y837) human induced pluripotent stem cells (iPSCs) were obtained from WiCell (Madison, WI, USA) and from Coriell Institute of Medical Research (Camden, NJ, USA) repositories, respectively. Cells were maintained and differentiated as previously mentioned (Patel et al. 2017). Undifferentiated iPSCs were seeded at a density of 2×10^4 cells/cm^2 and maintained in Essential-8 Medium (Life Technologies, Thermofisher, Waltham, MA) and grown on a Matrigel-coated (Trevigen, Gaithersburg, CT) tissue culture plastic surface (TCPS) for 5 days prior to differentiation. BMEC differentiation was obtained by following the protocol of Shusta and colleagues(Lippmann et al. 2014) and achieved by growing undifferentiated iPSCs in unconditioned media (UMM: DMEM/ F12 with 15 mM HEPES supplemented with 20% KO serum replacement, 1% MEM non-essential amino acids, and 0.5% Glutamax I (ThermoFisher, Waltham, MA, USA), and 0.1 mM β-mercaptoethanol (Sigma–Aldrich, St Louis, MO, USA)) for 6 days, with medium changed daily. After 6-day treatment, iPSC-derived BMECs were incubated in EC^{++} (EC serum-free medium (ECSFM, Thermofisher), supplemented with 1% platelet-poor derived plasma serum (PDS, Thermofisher), 20 µg/mL human basic fibroblast growth factor (R&D Systems) and 10 µM all-trans retinoic acid (Sigma–Aldrich)) for 2 days. Maturing BMECs were enzymatically dissociated by Accutase® (Corning, Corning, NY) treatment and seeded on TCPS and Transwell® inserts (Corning, polyester membrane, 0.4µ m pore size) coated with collagen from human placenta (Sigma) and fibronectin from bovine plasma (Sigma- Aldrich) at concentrations of 80 and 20 µg/cm^2, respectively. Cells were allowed to recover for 24 h and were incubated in EC$^-$ (ECSFM supplemented with 1% PDS) for another 24 h. All experiments were carried out by day 10 of differentiation.

iPSC differentiation into astrocytes and neurons were obtained following our previous differentiation protocol (Patel et al. 2017). In brief, undifferentiated iPSCs were differentiated into neural stem cells (NSCs) by 10 days of induction in the presence of neural induction medium (NIM, Life Technologies), followed by reseeding and maturation into neural progenitor cells (NPCs) by incubating such cells in the presence of neural differentiation medium (NDM) for 5 days. Differentiation of these NPCs into astrocytes was achieved by incubating NPCs on Matrigel® supplemented with astrocyte medium (AMM, Life Technologies) for 15 days, whereas differentiation into neurons was achieved by incubating cells on laminin/poly-D-lysine (Sigma–Aldrich) supplemented with neural maturation medium (NMM: Neurobasal Plus Medium (Life Technologies) supplemented with 1% CultureOne (Life Technologies)). Medium was changed every two days for up to 15 days.

Barrier Function and Co-culture Experiments

BMEC monolayer tightness was measured by assessing the transendothelial electrical resistance (TEER) using an EVOM STX2 chopstick electrode (World Precision Instruments, Sarasota, FL, USA). TEER was measured in three different locations on the insert, averaged, and subtracted from values obtained in blank inserts.

TEER values obtained at the beginning of experiments served as baseline value (Supplementary Fig. 1). Paracellular permeability was assessed by incubating inserts in the presence of 1 µM fluorescein solution (Sigma) added in the donor (top) chamber. Diffusion of fluorescein across monolayers was assessed by sampling 100 µL of the receiver (bottom) chamber every 15 min for 60 min. Fluorescence was assessed using a Synergy MX2 ELISA plate reader (Bio-Tek Instruments, Burlington, VT, USA).

Paracellular permeability across BMEC monolayers was performed by replacing the apical medium with [^{14}C]-mannitol (0.4 µCi/mL. 17.5 µM total concentration. Perkin-Elmer, Waltham, MA) and sampled at similar timepoints and sample volumes than fluorescein assay. Radioactivity in samples were determined by mixing samples in the presence of ScintiSafe® liquid scintillation cocktail (ThermoFisher) and quantified counted using a Beckman-Coulter LS6500 liquid scintillation counter (Beckman-Coulter, Pasadena, CA). Permeability (Pe) values to fluorescein were determined using the clearance-slope method as previously described (Perriere et al. 2005; Patel et al. 2017). Co-culture experiments were obtained by seeding day 8 BMECs on Transwell inserts juxtaposed over astrocytes/neurons wells. The apical chamber was maintained in EC medium, whereas the basolateral chamber was maintained in AMM (astrocytes) or NMM (neurons), respectively. Medium was changed in both chambers at day 9 and day 10 of BMECs differentiation timeline. Experiments were initiated at Day 10 of BMEC differentiation. Maximum TEER and average permeability values reported in BMEC monolayers can be found in Supplementary Table 1.

Immunofluorescence

Cells were quickly washed with ice-cold PBS and fixed in 4% paraformaldehyde (PFA, Electron Microscopy Sciences, Hatfield, PA, USA) and blocked for 30 min at room temperature in the presence of PBS supplemented with 10% goat serum (Thermofisher) supplemented with 0.2% Triton-X100 (Sigma). Cells were incubated overnight at 4 °C in primary antibodies (Supplementary Table 2) diluted in 10% goat serum and labeled with Alexa Fluor® 555-conjugated secondary antibodies for 1 h at room temperature (see Supplementary Table 1). Cells were observed at 200X magnification (20X long-distance dry objective) and acquired using a Leica DMi-8 inverted epifluorescence microscope (Leica Microsystems, Wetzlar, Germany). Images were processed using ImageJ (Image J, NIH, Bethesda, MD). Relative fluorescence was quantified using the built-in function in ImageJ.

Pharmacological Treatment

In experiments involving prolyl hydroxylase domain (PHD) inhibitors, HIF-1 stabilization in ambient air was chemically induced by treatment with 100µM dimethyloxalylglycine (DMOG) or FG-4592 (Cayman Chemicals, Ann Arbor, MI) for 24 h in DMEM-. Cells treated with DMEM- supplemented with 0.1% DMSO (GD) were used as controls. In experiments involving HIF inhibition, cells were exposed to DMEM- supplemented with 10 µM CAY10585 (Cayman Chemicals) or 10µM YC-1 (Cayman Chemicals) and immediately incubated into the hypoxic chamber set at 1% for 6 h. Cells treated with 0.1% DMSO served as vehicle. Following OGD stress, cells were allowed to reoxygenate in the absence of pharmacological inhibitors. In experiments involving VEGF inhibition, cells undergoing reoxygenation were immediately treated in the presence of 10µM sorafenib (Selleck Chemicals, Houston, TX) or 10µM sunitinib (Selleck Chemicals) for 18 h. Cells treated with 0.1% DMSO served as vehicle controls.

Enzyme-Linked Immunosorbent Assays (ELISA)

HIF-1α (Abcam, Cambridge, MA, USA) and VEGF (R&D Systems, Minneapolis, MN, USA) protein levels were determined by ELISA following the manufacturer's protocol. In brief, conditioned medium was collected and frozen at − 80 °C upon analysis for secreted VEGF levels. For HIF-1α collections, BMEC monolayers were washed with ice-cold PBS and treated with homogenization buffer supplemented with proteases inhibitor cocktail (Thermofisher) as recommended by the manufacturer. Cell homogenates were centrifuged, and supernatants were recovered and stored in − 80 °C upon ELISA analysis. HIF-1α protein levels were normalized to samples total protein content determined by BCA assay (Thermofisher).

MTS Assay

Cell metabolic activity was assessed on cells grown on a 96-well plate by an MTS-based CellTiter 96 Aqueous Assay (Promega, Madison, WI, USA) following the manufacturer's protocol. Briefly, concentrated MTS reagent was added to cells at a final dilution rate of 1:20 and allowed to react for 1 h. Cell media was recovered, followed by a measurement of absorbance at 490 nm using the Synergy MX2 ELISA plate reader (Bio-Tek). MTS reagent incubated

in unconditioned media (cell-free medium) served as the blank. Absorbance from blank samples was subtracted from cell samples. Optical density (OD) values in cells following treatment were normalized against OD values obtained in control (untreated) cells.

Statistics

All experiments were performed using at least three independent biological replicates (three independent passages and cell differentiation). Data are represented as mean ± SD. Statistical analysis was performed using Student's *t* test (control versus 24 h of OGD) or one-way analysis of the variance (ANOVA) complemented by a Dunnett post hoc analysis. $P < 0.05$ was considered statistically significant.

Results

Prolonged Oxygen-Glucose Deprivation Displays Different Outcomes in iPSC-Derived BMECs

In order to demonstrate a similar response than reported in our previous report (Page et al. 2016), iPSC-derived BMEC monolayers were challenged to prolonged (24 h) oxygen-glucose deprivation (OGD) stress and compared to hCMEC/D3 monolayers (Fig. 1). All three groups showed a significant decrease in TEER (Fig. 1a), however, CTR90F- and CTR65M-BMECs showed 50% decrease in TEER, contrasting with the 80% decrease observed in hCMEC/D3. Such results were confirmed by an increase in fluorescein permeability (Fig. 1b). Loss of barrier integrity was accompanied by a loss in tight junction complexes' integrity following prolonged OGD stress (Fig. 1c). CTR90F-derived BMECs showed a significant decrease in both claudin-5 and occludin immunoreactivity compared to their normoxic controls. In contrast, CTR65M-derived BMEC monolayers showed a robust immunoreactivity to both claudin-5 and occludin in both normoxic and OGD groups. In conclusion, these results suggest a differential response to prolonged OGD stress between CTR90F and CTR65M iPSC-derived BMECs.

iPSC-Derived BMECs Show Differences in Cell Metabolic and VEGF Secretion Levels During Prolonged OGD Stress

To better understand the differences between BMEC monolayers, we investigated changes in cell metabolic activity using MTS assay (Fig. 1d). Prolonged OGD stress resulted in a significant decrease in cell metabolic activity in all three cells. However, such decrease was less accentuated in iPSC-derived BMECs compared to hCMEC/D3 monolayers. Such decrease was unlikely due to decrease in glucose uptake, as immunoreactivity of glucose transporter 1 (GLUT1) remained similar or higher than normoxic controls (Fig. 1e). Finally, changes in secreted VEGF-A were assessed in BMEC monolayers following prolonged OGD stress (Fig. 1f), as VEGF-A constitutes an important hypoxia-induced growth factor documented to exert an hyperpermeable growth factor at the BBB (Al Ahmad et al. 2009; Chi et al. 2008; Vogel et al. 2007; Kilic et al. 2006; Fischer et al. 2002, 1999; Schoch et al. 2002; Zhang et al. 2000). Normoxic cells displayed similar secreted VEGF-A levels (250–380 pg/mL). Prolonged OGD stress resulted in an increase in VEGF in all three groups. Interestingly, both hCMEC/D3 and CTR65F-BMECs showed a 50% and 100% increase in VEGF secretion, whereas CTR90F-BMECs showed almost a 200% increase. Taken together, these results suggest that iPSC-derived BMECs are capable to respond to prolonged OGD stress similarly than hCMEC/D3 cells.

Differential Response to Prolonged OGD Stress Occurs in iPSC-Derived Astrocytes and Neurons

Following the results obtained in iPSC-derived BMECs monolayers were also reproduced in other cell types of the neurovascular unit, astrocytes and neurons monocultures were differentiated from the same iPSC lines and exposed to prolonged OGD stress (Supplementary Fig. 1). Prolonged OGD stress significantly reduced cellular metabolic activity in both astrocytes (Fig. S1A) and neurons (Fig. S1B). Although no particular difference between CTR90F and CTR65M-derived astrocytes was noted, cell metabolic activity in CTR90F-derived neurons appeared lower compared to CTR65M-derived neurons. Astrocytes showed an increase in VEGF-A secreted levels following OGD stress, in agreement with the literature (Al Ahmad et al. 2011; Al Ahmad et al. 2009; Schmid-Brunclik et al. 2008; Engelhardt et al. 2015; Margaritescu et al. 2011). Notably, CTR90F-astrocytes showed higher VEGF levels than CTR65M astrocytes. Such levels were significantly higher than neurons (Fig. S1D). Prolonged OGD stress significantly injured iPSC-derived neurons, as a decrease in neurite density was observed in both neuron monocultures (Fig. S1F). In conclusion, iPSC-derived astrocytes and neurons respond to prolonged OGD stress similarly as reported in the literature.

iPSC-Derived BMECs Show a Differential Response to OGD/Reoxygenation Stress

To assess the relevance of these cells as a putative hypoxic/ischemic in vitro model of the human BBB, cells were challenged to 6 h of OGD stress, followed by 18 h of reoxygenation (Fig. 2). Treatment with OGD/reoxygenation resulted in a decrease in TEER in both hCMEC/D3 and CTR90F

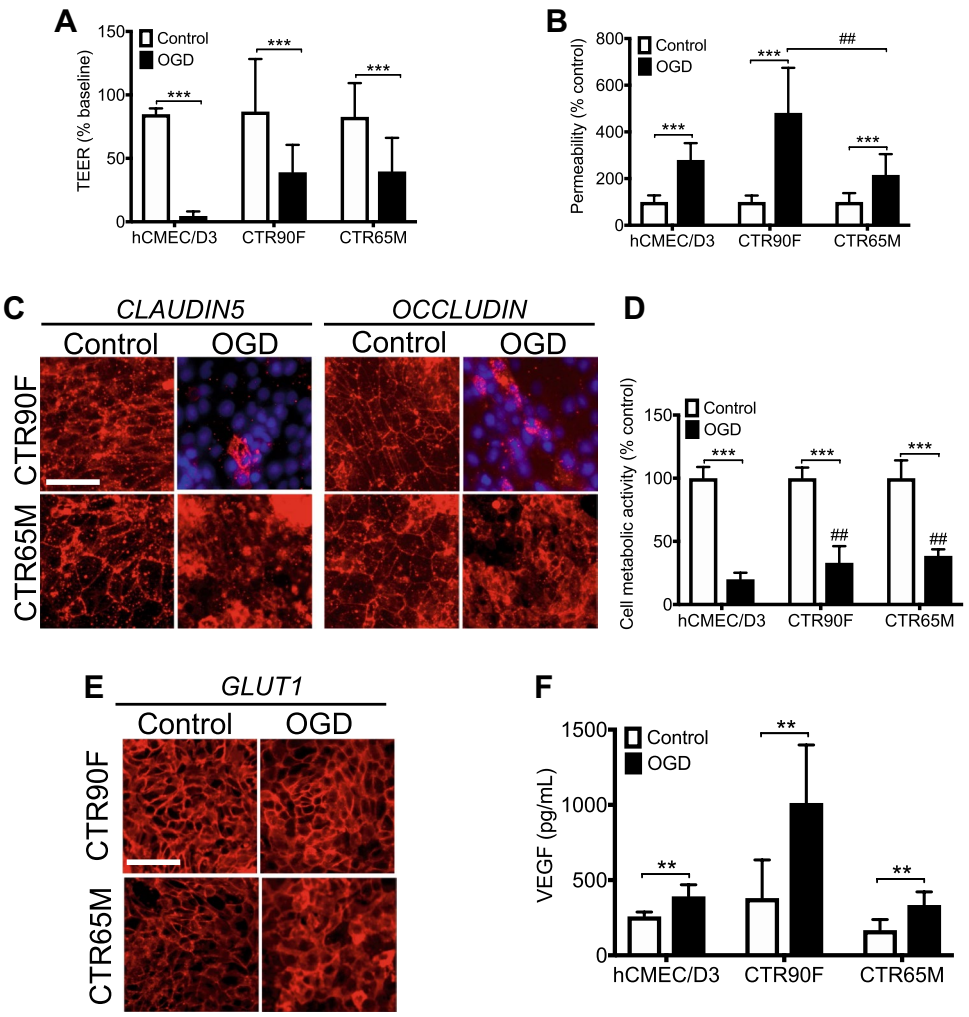

Fig. 1 Impact of prolonged oxygen-glucose deprivation stress on barrier function in iPSC-derived BMECs. Cells were exposed to prolonged oxygen-glucose deprivation (OGD) stress by exposing cells to glucose-free DMEM for 24 h in the presence of a hypoxic environment. **a** TEER and **b** sodium fluorescein permeability measurement in iPSC-derived BMECs and hCMEC/D3. **c** Representative micrograph pictures of claudin-5 and occludin in CTR90F and CTR65M-derived BMECs following 24 h of OGD stress. Note the quasi-absence of immunoreactivity in CTR90F-BMECs during OGD compared to CTR65M despite the presence of cell nuclei (DAPI, blue). Scale bar = 50 µm. **d** Change in cell metabolic activity by MTS assay. Note the higher metabolic rate in iPSC-derived BMECs compared to hCMEC/D3 in the OGD group. **e** GLUT1 expression profile in CTR90F and CTR65M-derived BMECs. Not the relative absence of changes in GLUT1 expression after 24 h of OGD. **f** VEGF secretion levels between controls and 24 h of OGD. VEGF levels were quantified from conditioned cell medium. Note the spike in VEGF levels in CTR90F-BMECs. * and ** denote $P < 0.05$ and $P < 0.01$ versus control, # and ## denote $P < 0.05$ and $P < 0.01$ versus hCMEC/D3, respectively

(Fig. 2b) following OGD stress, whereas no changes in TEER were observed in CTR65M-derived BMEC monolayers. Reoxygenation failed to restore the barrier function to values similar to controls in both hCMEC/D3 and CTR90F cell lines, whereas CTR65M maintained a barrier function similar to their normoxic controls. Similar outcomes were observed using paracellular tracers including fluorescein (Fig. 2c) and [^{14}C]-mannitol (Supplementary Fig. 2). To correlate changes in the barrier function to changes in tight junction integrity, immunofluorescence experiments were performed against claudin-5 and occludin (Fig. 2d and f). Both CTR90F and CTR65M showed a decrease in claudin-5 immunoreactivity and relative protein levels after 6 h of OGD compared to normoxic controls (Fig. 2d and e). However, during the reoxygenation phase, CTR65M showed a better claudin-5 outcome than CTR90F, both in protein localization and expression levels. In contrast, occludin (Fig. 2e) was lesser affected by OGD treatment than claudin-5. Semi-quantitative analysis (Fig. 2f) suggested an increase in occludin expression levels in both CTR90F and CTR65M compared to control. Reoxygenation mildly decreased occludin protein localization and expression in CTR90F but not in CTR65M. In conclusion, these results suggest a difference in barrier function integrity between

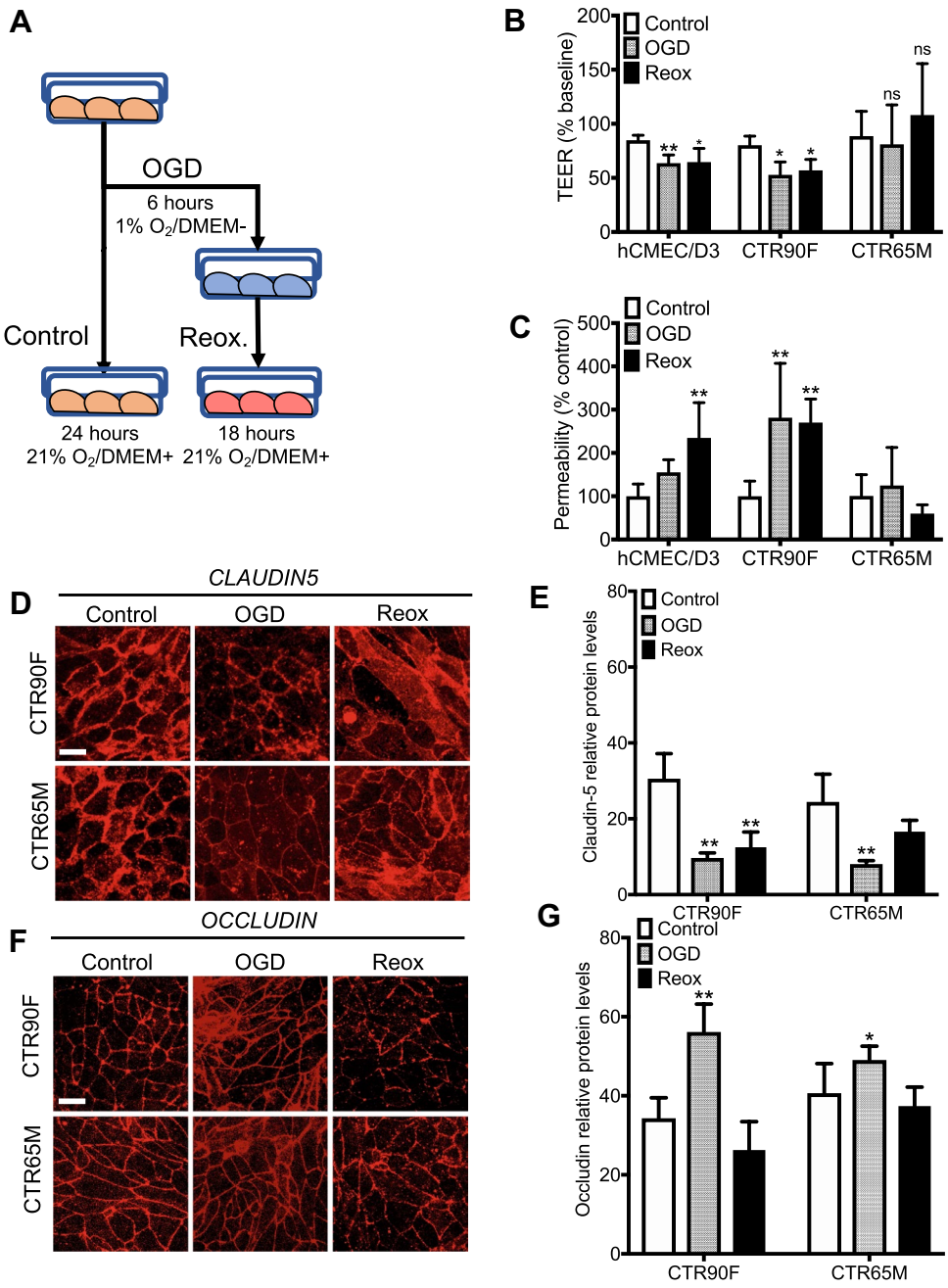

Fig. 2 Reoxygenation is a critical event in OGD-induced barrier disruption. **a** Sketch of the experimental design. Cells are incubated in OGD (glucose-free DMEM, 1% O2) for 6 h followed by reoxygenation for 18 h at ambient O_2 level (21%) in the presence of DMEM with D-glucose (5.5 mM). Cells maintained in DMEM with 5.5 mM D-glucose for 24 h. **b** TEER measurements in BMEC monolayers. TEER values at 6 h and 24 h (18 h of reoxygenation) were normalized to the TEER values recorded at 0-h timepoint. **c** Fluorescein permeability values at 6 h of OGD and 18 h of reoxygenation were normalized against the average permeability values measured in control groups. **d** and **e** Representative micrograph pictures of claudin-5 and occludin following OGD and reoxygenation. Note the decrease in claudin-5 immunoreactivity after 6 h of OGD indicative of an impaired barrier function, such decrease was more accentuated in CTR90F compared to CTR65M. Reoxygenation process appears as a major stressor on BMEC monolayers integrity as we not an important cytosolic localization of claudin-5 compared to control in CTR90F-BMECs. Scale bar = 50 µm. * and ** denote $P < 0.05$ and $P < 0.01$, respectively, versus control

CTR90F and CTR65M suggesting that such differences maybe partially explained by a differential maintenance of the barrier function.

iPSC-Derived BMECs Show a Differential Cellular Response to OGD/Reoxygenation Stress

As HIF-1 pathway constitutes an important pathway involved in the BBB response to hypoxia/ischemia in vitro and in vivo, changes in HIF-1 activity in this model were assessed by measuring changes in HIF-1α and VEGF. Under normoxic condition, both iPSC-derived BMECs showed HIF-1α protein levels higher than hCMEC/D3 (Fig. 3a). However, both iPSC-BMECs showed lower HIF-1α protein levels compared to hCMEC/D3 upon exposure to OGD stress (Fig. 3b). OGD stress decreased GLUT1 immunoreactivity in both iPSC-BMECs, and appeared more accentuated in CTR65M-BMECs, such changes in expression correlated with changes in cell metabolic activity (Fig. 3d). Finally, both hCMEC/D3 and iPSC-derived BMECs were capable to increase secreted

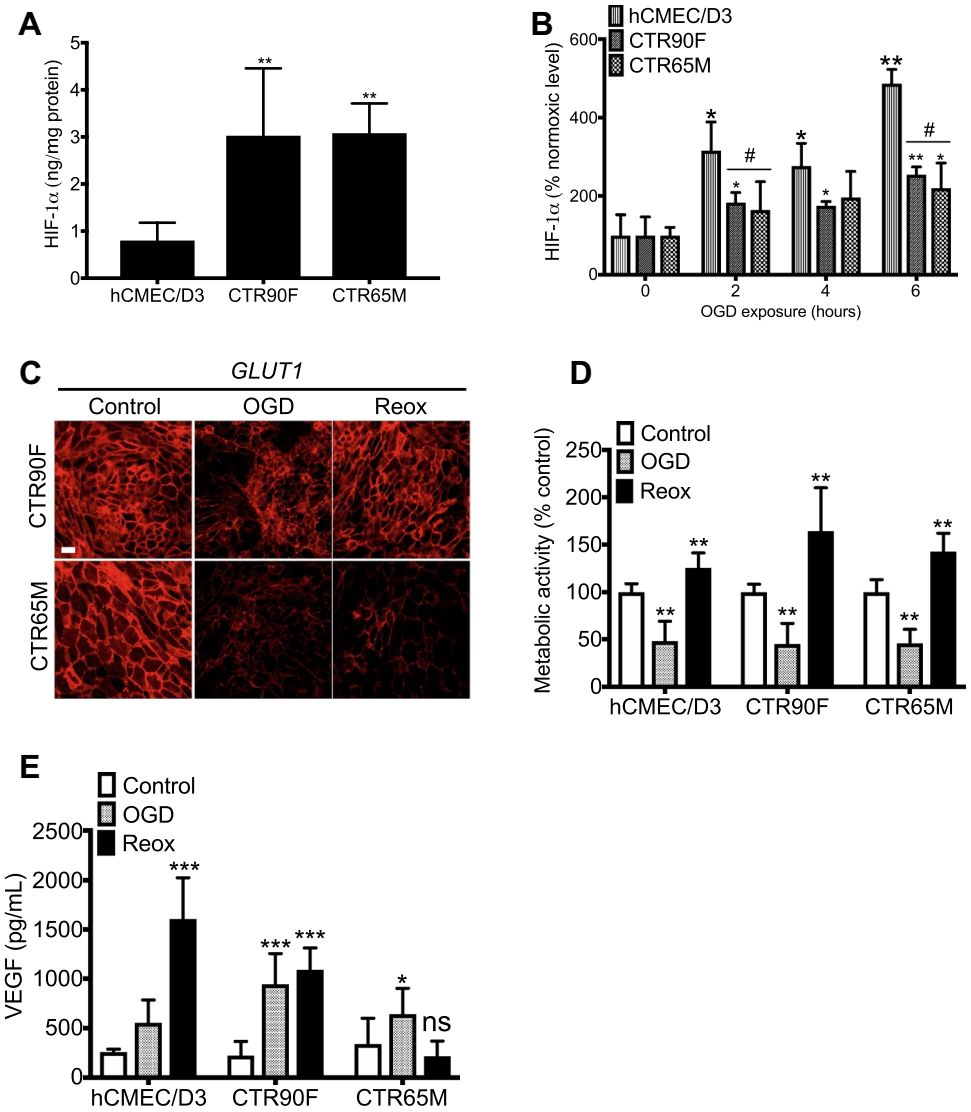

Fig. 3 OGD induces HIF-1α activation and VEGF expression in iPSC-derived BMECs. **a** HIF-1α protein levels under normoxic conditions. Cells were treated with DMEM + for 24 h under ambient O_2 level (21%). Total proteins were extracted and HIF-1α levels were determined by ELISA and normalized to total protein content in cell homogenates. Note the higher basal HIF-1α levels in CTR90F and CTR65M compared to hCMEC/D3. **b** HIF-1α stabilization level profile in BMECs following OGD stress. Note the overall increase in HIF-1α level in hCMEC/D3 that is higher than iPSC-derived BMECs. **c** Representative micrograph pictures of GLUT1 expression profile in CTR90F and CTR65M following OGD and reoxygenation. Note the decrease in GLUT1 expression in CTR65M monolayers. Scale bar = 100 µm. **d** Cell metabolic activity profile in BMECs following OGD and reoxygenation exposure. Cells were incubated for 2 h in the presence of MTS reagent. Absorbance values were normalized to values obtained in normoxic controls. Note the higher level during reoxygenation suggesting an increased mitochondrial activity. **e** VEGF levels in cell supernatants. The shorter incubation time (6 h) of OGD was included and compensated in the calculation of VEGF levels. Note the difference in VEGF expression profile between CTR90F and CTR65M

VEGF levels upon and after OGD stress, with CTR65M-derived BMECs showing the lowest VEGF increase from all three groups. Taken together, iPSC-derived BMECs respond to OGD stress via activation of the HIF-1 pathway.

iPSC-Derived Astrocytes and Neurons Show a Differential Cellular Response to OGD/Reoxygenation Stress

In addition to changes in iPSC-derived BMECs, this study documented changes in iPSC-derived astrocytes and neurons following OGD/reoxygenation stress (Supplementary Fig. 3). OGD/reoxygenation had little impact on CTR90F

and CTR65M-derived astrocyte cell metabolic activity (Fig. S3A), whereas a difference in HIF-1α protein levels was observed between CTR90F-astrocytes and CTR65M-astrocytes (Fig. S3B). Such differences were reflected in VEGF secretion levels, as CTR90F-astrocytes displayed higher VEGF levels than CTR65M-astrocytes (Fig. S3C). CTR90F-derived neurons showed a significant decrease following OGD and maintained such low cell metabolic activity during reoxygenation (Fig. S3D), whereas CTR65M-derived neurons cell metabolic activity was mildly decreased. Notably, OGD treatment showed a differential response in neurites depletion between CTR90F neurons and CTR65M neurons (Fig. S3E and F), as CTR65M neurons showed a sustained neurite density similar to control.

However, reoxygenation dramatically blunted neurites density in both groups, highlighting the susceptibility of these cells to OGD/reoxygenation stress. In conclusion, iPSC-derived astrocytes and neurons were capable to respond to OGD/reoxygenation stress in similar fashion than reported in the existing literature.

HIF-1 Activation by Prolyl-4-Hydroxylase Inhibitors Shows a Differential Response Between iPSC-Derived BMECs

To determine the influence of HIF-1α effect on the barrier function in iPSC-derived BMEC monolayers, cells were exposed to glucose-free medium under normoxic condition and exposed in the presence of 100μM dimethyloxalylglycine (DMOG) or FG-4592 (Roxadustat®), two distinct prolyl-4-hydroxylase domain (PHD) inhibitors (Besarab et al. 2015; Elvidge et al. 2006) (Fig. 4).

Glucose deprivation (GD) had little impact on HIF-1α proteins (Fig. 4a) in hCMEC/D3 monolayers, whereas a significant increase was observed both CTR90F- and CTR65M-BMECs. The presence of PHD inhibitors was necessary to induce an increase in HIF-1α protein levels in hCMEC/D3 monolayers (Fig. 4b), whereas such treatment had a marginal effect on HIF-1α in iPSC-derived BMECs. Interestingly, 24 h of treatment with DMOG or FG-4592 resulted in a decreased GLUT1 immunoreactivity in CTR90F-derived BMEC monolayers (Fig. 4c), whereas it showed an increased immunoreactivity in CTR65M cells. However, treatment with DMOG or FG-4592 failed to show significant differences in cell metabolic activity as measured by MTS (data not shown). Finally, changes in secreted VEGF levels were determined following treatment with PHD inhibitors (Fig. 4d). Notably, glucose deprivation alone yielded to lower VEGF levels compared to normoxic/normoglycemic controls in both iPSC-derived BMEC monolayers. Treatment with DMOG or FG-4592 yielded to a significant increase in VEGF production in CTR90F-BMECs, whereas CTR65M-BMECs displayed an increase only in FG-4592 treated group. In conclusion, iPSC-derived BMEC monolayers are capable to respond to PHD inhibitors treatment by increasing HIF-1 activity under normoxic condition.

Prolyl Hydroxylase Inhibition by Small Molecules Increased BMECs Permeability via a Selective Targeting of Claudin-5 Pathway

To show a correlation between HIF-1α activation and changes in the barrier function, BMEC monolayers were treated with either DMOG or FG-4592 for 24 h, following assessment of the barrier function using TEER and fluorescein permeability (Fig. 4e and f). No differences in TEER were noted in treated groups (Fig. 4e), albeit an increase in fluorescein permeability (Fig. 4f) was noted following DMOG or FG-4592 treatment. Such changes in the barrier function were associated with changes in tight junction complexes integrity (Fig. 4g and h), as treatment with DMOG and FG significantly affected claudin-5 levels, whereas no major changes in occludin were noted in both cells following treatment. In conclusion, activation of the HIF pathway by PHD inhibitors resulted in a decreased barrier function. Such decrease may be attributed to a selective loss in claudin-5 expression. In conclusion, an increase in HIF-1 activity did partially correlate with loss of tight junction complexes.

HIF-1 Inhibition by Small Molecules During OGD Stress Inhibits VEGF Production in BMEC Monolayers

To demonstrate the relevance of targeting the HIF-1 pathway on OGD-induced barrier disruption, BMECs were exposed to OGD stress in the presence of 10 μM CAY10585 or 10 μM YC-1 (Zhang et al. 2013; Lee et al. 2007; Chun et al. 2001; Chen et al. 2015; Engelhardt et al. 2014a; Yan et al. 2011; Yeh et al. 2007), and allowed to reoxygenate in the absence of such HIF-1 inhibitors (Fig. 5). Treatment with HIF-1 inhibitors was sufficient to decrease significantly HIF-1α protein levels in hCMEC/D3 levels (Fig. 5a), but mildly affected HIF-1α protein levels in CTR90F and CTR65M-BMECs. However, such treatment resulted in a significant decrease in GLUT1 immunoreactivity (Fig. 5b), and such decrease was more sustained in CTR90F than CTR65M. Yet, such decrease in GLUT1 expression had only a minor effect on cell metabolic activity, with a small but significant decrease cell metabolic activity following treatment with YC-1 (Fig. 5c). Treatment with HIF-1 inhibitors during OGD were sufficient to decrease VEGF secretion (Fig. 5d) by 50% in both hCMEC/D3 and CTR90F-derived BMECs; however, no differences in CTR65M-derived cells. In summary, HIF-1 inhibitors were capable to partially inhibit HIF/VEGF axis in iPSC-derived BMECs following OGD stress.

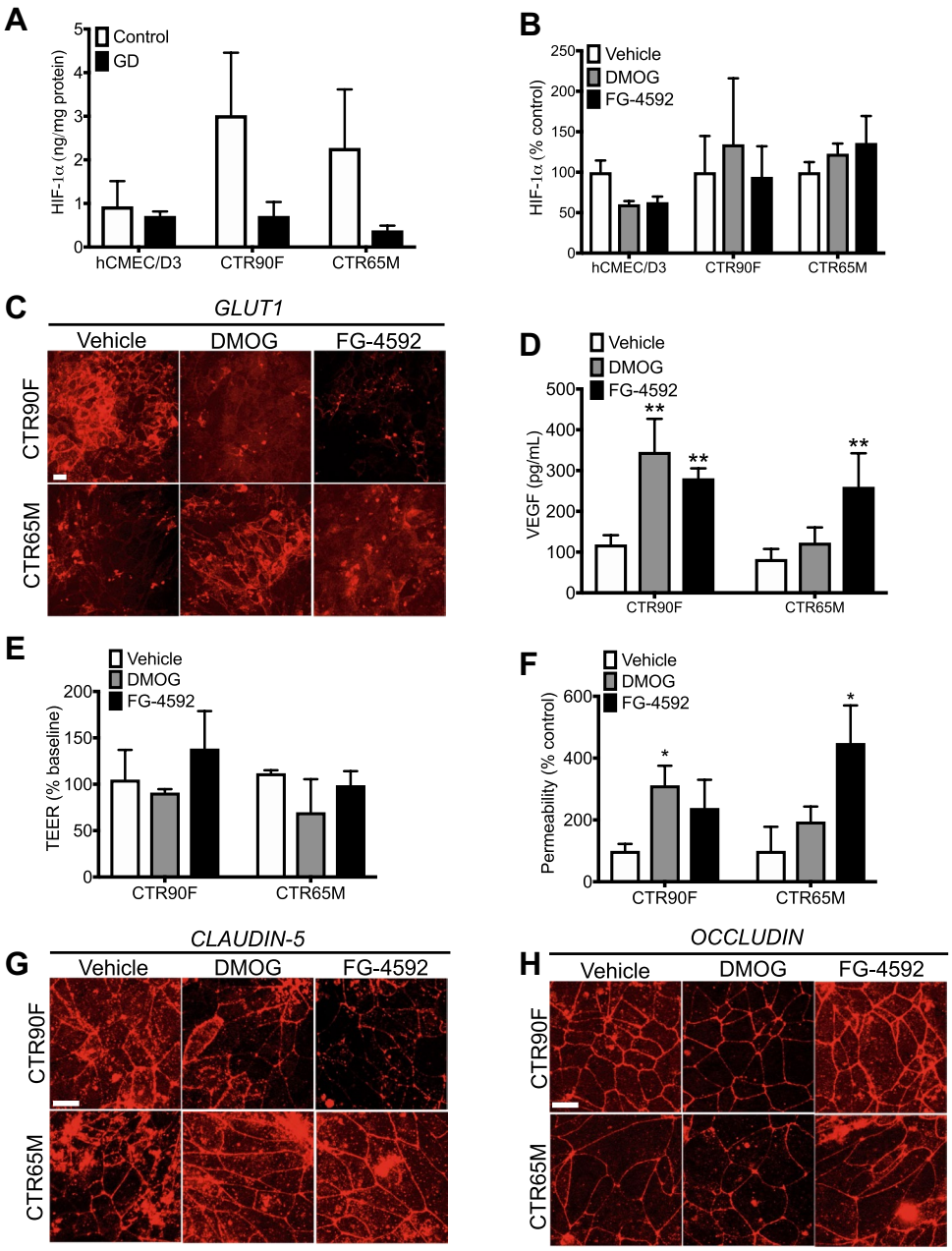

Fig. 4 HIF-1 activation by PHD inhibitors mildly impacts BMEC monolayer integrity. Cells were maintained for 6 or 24 h in glucose-free medium under normoxic condition, in the presence of 100μM DMOG or FG-4592. **a** Effect of glucose-free media on HIF-1α protein levels. Cells were incubated for 6 h in glucose-free medium under ambient atmosphere. Note the decrease in HIF-1α protein levels in CTR90F and CTR65M-derived BMEC monolayers. **b** Effect of DMOG and FG-4592 on HIF-1α protein levels. Cells were treated for 6 h in the presence of 100μM DMOG or FG-4592, cells treated with 0.1% DMSO served as control. Note the absence of HIF-1α induction. **c** Representative GLUT1 immunocytochemistry micrograph pictures following 24 h of treatment. Scale bar = 50 μm. **d** VEGF levels following 24 h of treatment. Note the increase in VEGF levels following treatment with DMOG or FG-4592. **e** TEER values after 24 h of treatment. Control was arbitrarily set as 100%. Note the absence of effect on the barrier function. **f** Fluorescein permeability following 24 h of treatment. Note the increased permeability in both monolayers, such increase reflects changes in VEGF levels observed following similar treatment. **g** and **h** Immunocytochemistry micrograph pictures of claudin-5 and occludin following 24 h of treatment. Scale bar = 50 μm. * and ** denote $P < 0.05$ and $P < 0.01$ versus vehicle

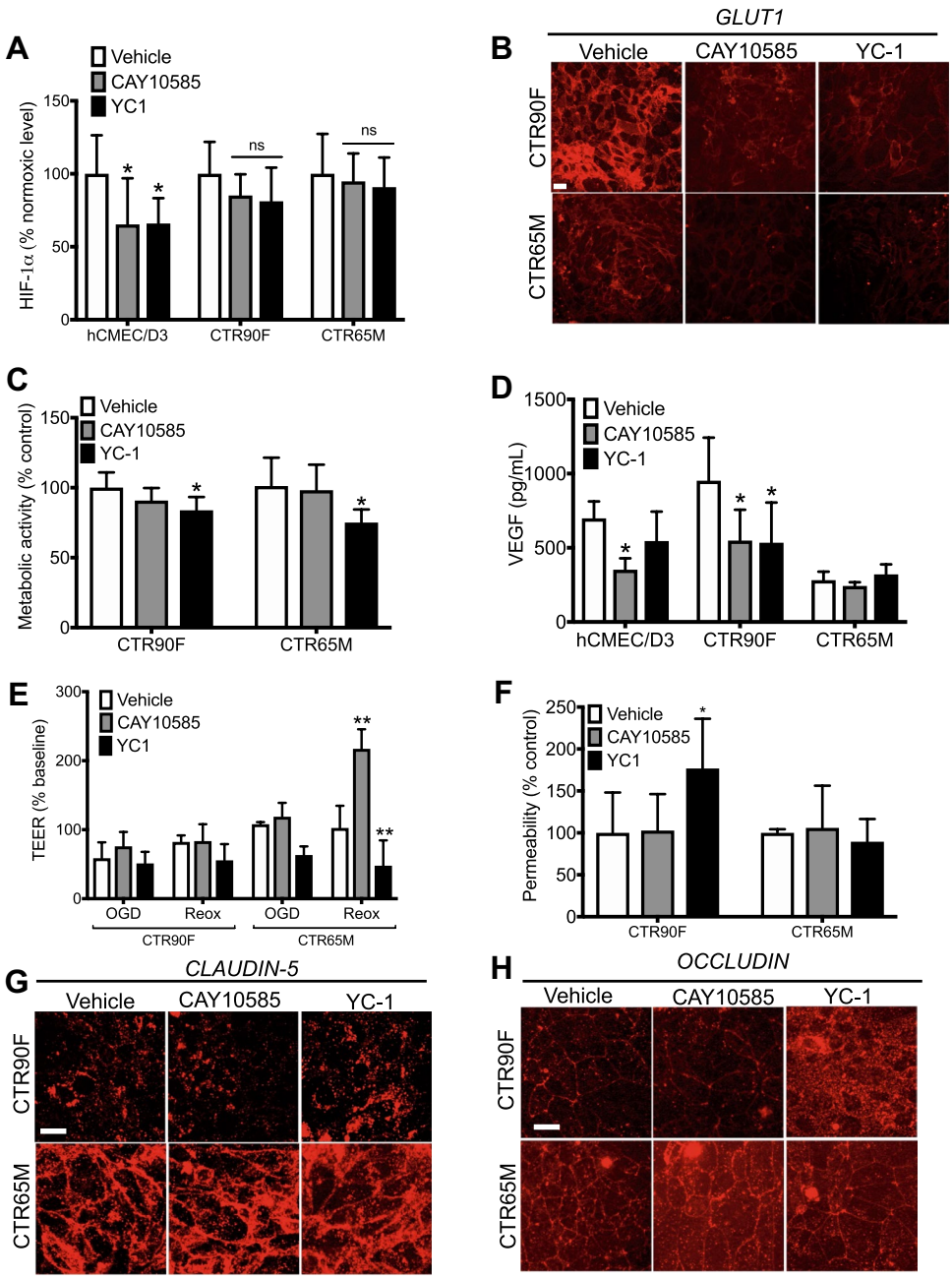

Fig. 5 HIF-1 inhibitor treatments do not improve the barrier function in BMEC monolayers. Cells were treated in the presence of 10µM CAY10585 or YC-1 during the OGD phase. Such inhibitors were absent during the reoxygenation phase. **a** Effect of HIF-1 inhibitors on HIF-1α protein levels. Note the absence of effects observed in iPSC-derived BMECs. **b** Representative GLUT1 immunocytochemistry micrograph pictures after 18 h of treatment. Scale bar = 50 µm. **c** Effect of HIF-1 inhibitors on cell metabolic activity during the reoxygenation phase. Note the decreased activity in YC-1 treated cells, suggesting a possible impaired metabolism. **d** VEGF levels after 6 h of OGD. Note the significant decrease in both hCMEC/D3 and CTR90F-BMECs. **e** TEER values after treatment (6 h of OGD and 18 h of reoxygenation). Cells were maintained without inhibitors during the reoxygenation phase. **f** Fluorescein permeability at 18 h of reoxygenation. **g** and **h** Immunocytochemistry micrograph pictures of claudin-5 and occludin following 24 h of treatment. Scale bar = 50 µm. * and ** denote $P < 0.05$ and $P < 0.01$ versus vehicle

HIF-1 Inhibition During OGD Stress Does Not Prevent OGD/Reoxygenation-Induced Barrier Disruption in iPSC-Derived BMEC Monolayers

To better associate the decrease in HIF/VEGF with changes in the barrier function, changes in the barrier function were assessed in iPSC-derived BMEC monolayers following treatment with CAY10585 or YC-1 immediately after OGD stress and following reoxygenation (Fig. 5e and f). Treatment with HIF-1 inhibitors (CAY10585 or YC-1) failed to improve TEER in BMEC monolayers both after OGD stress (Fig. 5e) and after reoxygenation. No differences in fluorescein permeability were noted (Fig. 5f).

Treatment with CAY10585 or YC-1 did not significantly alter the expression and localization of claudin-5 in both CTR90F and CTR65M. In contrast, treatment with YC-1 significantly altered occludin localization in CTR90F, whereas no changes were noted in CTR65M monolayers (Fig. 5g and h). In conclusion, HIF-1 inhibition by small molecules failed to improve the barrier function during and after OGD stress.

Anti-angiogenic Small Molecules Treatment Worsened the Barrier Function in iPSC-Derived BMECs During Reoxygenation Phase

VEGF constitutes an important hyperpermeable growth factor involved in hypoxia-induced blood–brain barrier disruption (Yan et al. 2012; Kanazawa et al. 2011; Al Ahmad et al. 2009; Kilic et al. 2006; Fischer et al. 2002; Schoch et al. 2002; Zhang et al. 2000). VEGF inhibition by small molecules has been associated with improved BBB function in animal models of cerebral ischemia (Kim et al. 2018, b; Greenberg and Jin 2013; Ke and Zhang 2013; Pikula et al. 2013; Margaritescu et al. 2011; Bauer et al. 2010), yet the relevance of such pathway in a clinical setting remains to be documented. Hence, we investigated the effect of two FDA-approved anti-angiogenic tyrosine kinase inhibitors (sorafenib (Nexavar®) and sunitinib (Sutent®)) (Roskoski 2017), known to inhibit VEGFR2 (Fig. 6). Treatment with 10µM sorafenib resulted in a significant decrease in cell metabolic activity in both CTR90F and CTR65M-BMECs compared to vehicle control group. In contrast, 10 µM sunitinib mildly affected cell metabolic activity. Treatment with sorafenib or sunitinib significantly decreased GLUT1 expression compared to vehicle (Fig. 6b). In addition to changes in GLUT1 and cell metabolic activity, changes in barrier function were reported following treatment with these two inhibitors (Fig. 6c and f). Treatment with sorafenib resulted in a dramatic disruption of the barrier function in both BMEC monolayers, as measured by a significant decrease in TEER (Fig. 6c) and increased fluorescein permeability (Fig. 6d). Noteworthy, CTR90F-derived BMECs displayed a higher susceptibility to sorafenib than CTR65M-derived BMECs. As expected, immunocytochemistry analysis of claudin-5 and occludin (Fig. 6e and f, respectively) showed a massive

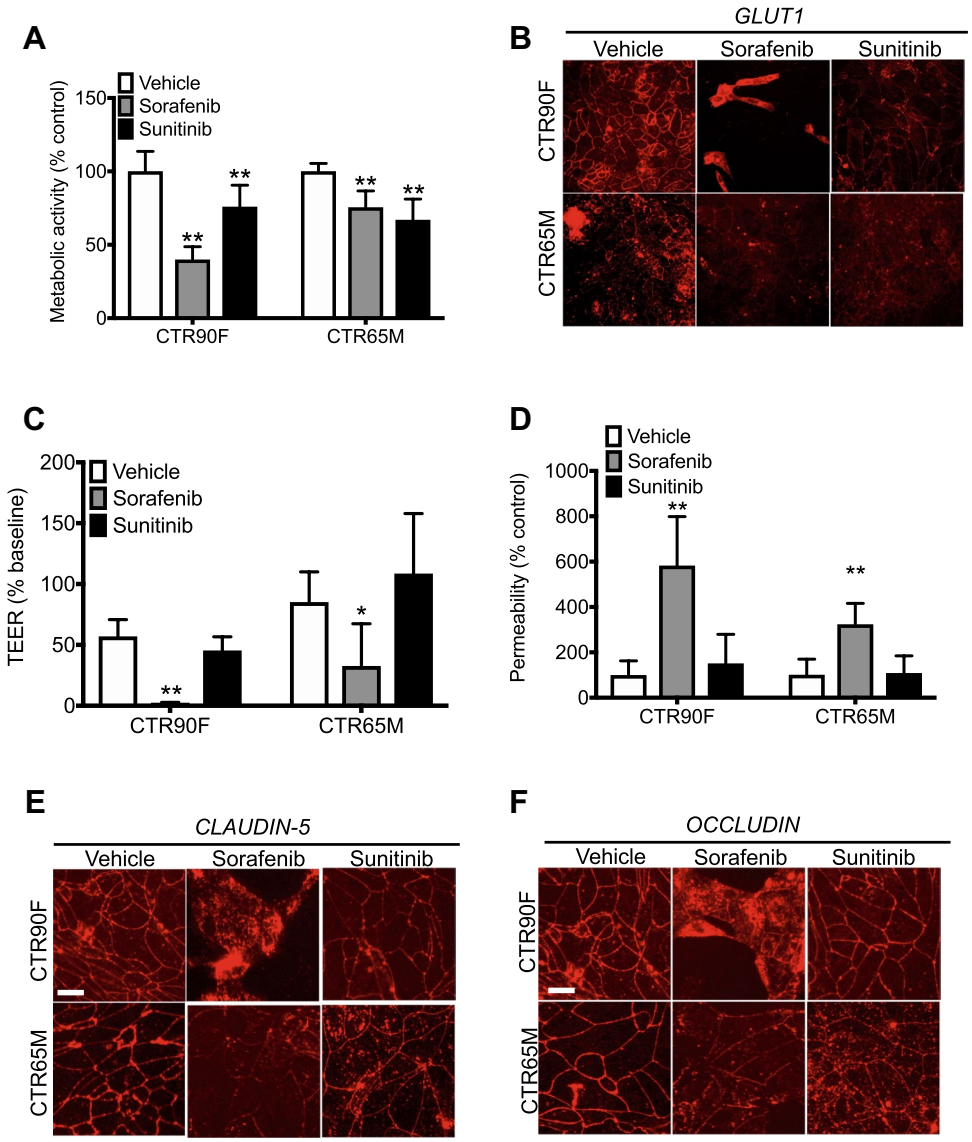

Fig. 6 VEGF inhibition by anti-angiogenic inhibitors impairs the barrier recovery. Cells were treated in the presence of 10µM sorafenib or sunitinib during the reoxygenation phase only. **a** Effect of sorafenib and sunitinib on BMECs cell metabolic activity after 18 h of reoxygenation. **b** Representative GLUT1 immunocytochemistry micrograph pictures after 18 h of treatment. Scale bar = 50 µm. **c** TEER values after treatment during the reoxygenation phase. **d** Fluorescein permeability at 18 h of reoxygenation. **e** and **f** Immunocytochemistry micrograph pictures of claudin-5 and occludin following 18 h of reoxygenation in the presence of sorafenib or sunitinib. Scale bar = 50 µm. * and ** denote $P < 0.05$ and $P < 0.01$ versus vehicle

disruption of the monolayer integrity with the presence of wide intercellular gaps. In conclusion, treatment with anti-angiogenic inhibitors significantly impaired the barrier recovery during reoxygenation.

Co-cultures Show a Differential Response to OGD/Reoxygenation Stress

Finally, we investigated changes in the barrier function in BMECs co-cultured with astrocytes or neurons (Supplementary Fig. 3). The presence of co-cultures exacerbated (Fig. S3A and B) BMECs response to OGD stress, in particular in CTR90F-BMECs. Reoxygenation failed to restore the barrier function in CTR90F co-cultures and resulted in worsened barrier function compared to monocultures, as seen with fluorescein permeability. As expected, CTR65M co-cultures showed no differences in terms of permeability. In contrast, neuron co-cultures showed no detrimental effects on TEER during OGD (Fig. S3C&D) and showed detrimental effects only during reoxygenation, whereas OGD/reoxygenation yielded to a fivefold increase in permeability in CTR90F co-cultures, whereas no differences were observed in CTR65M co-cultures. In conclusion, these results suggest that the presence of co-cultures (astrocytes or neurons) influences the barrier response following OGD/reoxygenation stress.

Discussion

Hypoxia/ischemia constitutes an important stress factor capable to disrupt the blood–brain barrier (BBB) function in several neurological diseases. Although several studies documented the cellular and molecular response of the BBB during hypoxic/ischemic insult using in vitro (Kokubu et al. 2017; Page et al. 2016; Engelhardt et al. 2014a; Zhu et al. 2012; Al Ahmad et al. 2009; Koto et al. 2007; Yang et al. 2007; Fischer et al. 2004, 2002, 1999; Abbruscato and Davis 1999) and in vivo approaches (Gussenhoven et al. 2019; Ma et al. 2017; Yang and Rosenberg 2011; Bauer et al. 2010; Lochhead et al. 2010; McCaffrey et al. 2009; Brown and Davis 2005; Witt et al. 2003; Mark and Davis 2002), such findings have yet to translate into clinically relevant targets. A major caveat of current in vitro models of the BBB is marked by their limited ability to form tight monolayers, in this study, we investigated the effect of oxygen-glucose deprivation (OGD) stress (an in vitro model of cerebral ischemia) on the barrier function in iPSC-derived BMEC monolayers, by exposing such cells to 6 h of OGD, followed by 18 h of reoxygenation in normoglycemic medium.

Such models were capable to reproduce hallmarks of existing in vitro models of cerebral hypoxia/ischemia by showing disrupted barrier function (decreased TEER, increased permeability to fluorescein and mannitol), partial loss of tight junction complexes. Such response occurred via the stabilization of HIF-1α and increased VEGF-A secretion.

Overall, both iPSC lines used in this study showed responses similar to those observed in hCMEC/D3 monolayers, a somatic adult immortalized human BMEC line (Weksler et al. 2005). All three cells showed disruption in the barrier function following prolonged (24 h) and acute (6 h) OGD stress, and all three cells showed increase in HIF-1α and VEGF following OGD stress. A major concern of the use of stem cells for modeling hypoxia/ischemia in vitro is their compliance to hypoxia (Mimeault and Batra 2013; Nobes et al. 1990; Medley et al. 2013; Mathieu et al. 2014; Lopez-Iglesias et al. 2015; Nakashima et al. 2018). This study is in agreement with our previous study (Page et al. 2016) and a recent by Kokubu and colleagues (Kokubu et al. 2017). Such data are in agreement with the existing literature and suggest that such BMECs, despite their stem cell origin, were capable to respond similarly to human BMECs obtained from somatic adult cells. Similar outcomes were reported in iPSC-derived astrocytes and neurons used in this study (Antoniou et al. 2011; Genetos et al. 2010; Lin et al. 2015; Martin-Aragon Baudel et al. 2017; Wang et al. 2012, 2015; Schmid-Brunclik et al. 2008), suggesting that the differentiation of iPSCs into different cell types of the neurovascular unit may allow such cells to respond to hypoxia/ischemia similarly than primary cells. However, further studies are necessary to ensure a more detailled characterization of these cells in order to demonstrate their ability to reflect similar cellular and molecular mechanisms as reported in primary cells. In our study, the increase in VEGF levels in both BMECs and astrocytes following hypoxic/ischemic injury was consistent with the literature (Mo et al. 2016; Wang et al. 2016a, b, 2007; Wu et al. 2015; Sajja et al. 2014; Ke and Zhang 2013; Margaritescu et al. 2011; Mani et al. 2010, 2005; Kim et al. 2008; Plaschke et al. 2008; Schmid-Brunclik et al. 2008; Fischer et al. 2002; Jin et al. 2002; Chow et al. 2001). In addition, we observed that the presence of astrocytes in our co-culture models yielded worsened barrier function compared to monocultures, in agreement with the existing literature (Al Ahmad et al. 2009; Brillault et al. 2002; Kuntz et al. 2014).

Yet, our study also failed to show a direct effect of HIF-1 on the barrier function following treatment with YC-1, in contradiction with some studies (Na et al. 2015; Yan et al. 2011; Yeh et al. 2007), but in agreement with two recent studies (Barteczek et al. 2017; Pikula et al. 2013). In those studies, deletion of HIF-1α and HIF-2α in mice failed to show differences in cerebral edema compared to wild-type, whereas serum VEGF levels in patients failed to correlate with increased white matter hyperdensity. Our study showed that the use of tyrosine kinase inhibitors (sorafenib, sunitinib) as anti-angiogenic agents failed to show improvement

of the barrier function during the reoxygenation phase. This finding agrees with a recent study reporting worsened cardiovascular outcomes in elders treated with such therapeutics (Jang et al. 2016). In addition, such results suggest the important function of pro-angiogenic pathways in this model, in agreement with the beneficial role of angiogenesis following stroke injury (Prakash and Carmichael 2015; Ruan et al. 2015; Yang et al. 2013; Greenberg and Jin 2013; Zhong et al. 2010; Ohab et al. 2006).

Finally, the major difference observed in this study is the differential response of the two iPSC lines following OGD stress, such differences were reflected in both astrocytes, BMECs and neurons. In particular, CTR65M appeared as a more compliant iPSC line than CTR90F to OGD/reoxygenation stress. It is important to note that until now, variability between iPSC lines in regard of in vitro BBB models was both our groups and others as discrete and minimal (Lee et al. 2018; Canfield et al. 2017; Al-Ahmad 2017; Vatine et al. 2017; Lim et al. 2017), as these BMECs showed similar outcomes in terms of BBB phenotype and barrier function. Several hypotheses may explain such differences. Our data showed some similarities in response between CTR90F (a female iPSC line) and hCMEC/D3 (originated from a female patient), whereas CTR65M displayed a distinct behavior. The effect of sex (chromosomal sex as a biological variable) at the BBB remains poorly understood at this time. Therefore, the inclusion of additional iPSC lines (from male and female patients) may help differentiate the effect of sex from other variables. Another hypothesis explaining such difference may inherent to the derivation process, in particular due to the random nature of the insertion of the four transcription factors, but also on clonal differences. Therefore, a side-by-side comparison of clones obtained from the same patient may help explain some aspect of this variability. Finally, we cannot exclude a possible genetic and epigenetic polymorphism inherent of each individual. Thus, a further analysis of gene variants may help explain differences observed in our study. In conclusion, our study suggests that iPSC-derived BMEC monolayers may be suitable for assessing changes at the BBB during hypoxia/ischemia following the validation of our findings into in vivo models and eventually be used as a platform for identifying novel target to restore the barrier function.

Acknowledgements S.P. and A.A. performed the experiments presented in this study. A.A. designed the study and wrote the manuscript.

Funding This study was funded by TTUHSC institutional funds and by a Laura W. Bush Institute for Women's Health seed grant to A.A.

Compliance on Ethical Standards

Conflict of interest The authors declare that they have no conflict of interest to disclose.

References

Abbruscato, T. J., & Davis, T. P. (1999). Combination of hypoxia/aglycemia compromises in vitro blood-brain barrier integrity. *Journal of Pharmacology and Experimental Therapeutics, 289*(2), 668–675.

Al Ahmad, A., Gassmann, M., & Ogunshola, O. O. (2009). Maintaining blood-brain barrier integrity: Pericytes perform better than astrocytes during prolonged oxygen deprivation. *Journal of Cellular Physiology, 218*(3), 612–622. https://doi.org/10.1002/jcp.21638.

Al Ahmad, A., Gassmann, M., & Ogunshola, O. O. (2012). Involvement of oxidative stress in hypoxia-induced blood-brain barrier breakdown. *Microvascular Research, 84*(2), 222–225. https://doi.org/10.1016/j.mvr.2012.05.008.

Al Ahmad, A., Taboada, C. B., Gassmann, M., & Ogunshola, O. O. (2011). Astrocytes and pericytes differentially modulate blood-brain barrier characteristics during development and hypoxic insult. *Journal of Cerebral Blood Flow & Metabolism, 31*(2), 693–705. https://doi.org/10.1038/jcbfm.2010.148.

Al-Ahmad, A. J. (2017). Comparative study of expression and activity of glucose transporters between stem cell-derived brain microvascular endothelial cells and hCMEC/D3 cells. *American Journal of Physiology-Cell Physiology, 313*(4), C421–C429. https://doi.org/10.1152/ajpcell.00116.2017.

Antoniou, X., Gassmann, M., & Ogunshola, O. O. (2011). Cdk5 interacts with Hif-1alpha in neurons: A new hypoxic signalling mechanism? *Brain Research, 1381*, 1–10. https://doi.org/10.1016/j.brainres.2010.10.071.

Barteczek, P., Li, L., Ernst, A. S., Bohler, L. I., Marti, H. H., & Kunze, R. (2017). Neuronal HIF-1alpha and HIF-2alpha deficiency improves neuronal survival and sensorimotor function in the early acute phase after ischemic stroke. *Journal of Cerebral Blood Flow & Metabolism, 37*(1), 291–306. https://doi.org/10.1177/0271678X15624933.

Bauer, A. T., Burgers, H. F., Rabie, T., & Marti, H. H. (2010). Matrix metalloproteinase-9 mediates hypoxia-induced vascular leakage in the brain via tight junction rearrangement. *Journal of Cerebral Blood Flow & Metabolism, 30*(4), 837–848. https://doi.org/10.1038/jcbfm.2009.248.

Besarab, A., Provenzano, R., Hertel, J., Zabaneh, R., Klaus, S. J., Lee, T., et al. (2015). Randomized placebo-controlled dose-ranging and pharmacodynamics study of roxadustat (FG-4592) to treat anemia in nondialysis-dependent chronic kidney disease (NDD-CKD) patients. *Nephrology Dialysis Transplantation, 30*(10), 1665–1673. https://doi.org/10.1093/ndt/gfv302.

Brillault, J., Berezowski, V., Cecchelli, R., & Dehouck, M. P. (2002). Intercommunications between brain capillary endothelial cells and glial cells increase the transcellular permeability of the blood-brain barrier during ischaemia. *Journal of Neurochemistry, 83*(4), 807–817.

Brown, R. C., & Davis, T. P. (2005). Hypoxia/aglycemia alters expression of occludin and actin in brain endothelial cells. *Biochemical and Biophysical Research Communications, 327*(4), 1114–1123. https://doi.org/10.1016/j.bbrc.2004.12.123.

Canfield, S. G., Stebbins, M. J., Morales, B. S., Asai, S. W., Vatine, G. D., Svendsen, C. N., et al. (2017). An isogenic blood-brain barrier model comprising brain endothelial cells, astrocytes, and neurons derived from human induced pluripotent stem cells. *Journal of Neurochemistry, 140*(6), 874–888. https://doi.org/10.1111/jnc.13923.

Chen, Y. F., Lin, Y. C., Chen, J. P., Chan, H. C., Hsu, M. H., Lin, H. Y., et al. (2015). Synthesis and biological evaluation of novel 3,9-substituted beta-carboline derivatives as anticancer

agents. *Bioorganic & Medicinal Chemistry Letters, 25*(18), 3873–3877. https://doi.org/10.1016/j.bmcl.2015.07.058.

Chi, O. Z., Hunter, C., Liu, X., & Weiss, H. R. (2008). Effects of deferoxamine on blood-brain barrier disruption and VEGF in focal cerebral ischemia. *Neurological Research, 30*(3), 288–293. https://doi.org/10.1179/016164107X230135.

Choi, K. H., Kim, H. S., Park, M. S., Kim, J. T., Kim, J. H., Cho, K. A., et al. (2016). Regulation of Caveolin-1 Expression Determines Early Brain Edema After Experimental Focal Cerebral Ischemia. *Stroke, 47*(5), 1336–1343. https://doi.org/10.1161/STROKEAHA.116.013205.

Chow, J., Ogunshola, O., Fan, S. Y., Li, Y., Ment, L. R., & Madri, J. A. (2001). Astrocyte-derived VEGF mediates survival and tube stabilization of hypoxic brain microvascular endothelial cells in vitro. *Brain Research Developmental Brain Research, 130*(1), 123–132.

Chun, Y. S., Yeo, E. J., Choi, E., Teng, C. M., Bae, J. M., Kim, M. S., et al. (2001). Inhibitory effect of YC-1 on the hypoxic induction of erythropoietin and vascular endothelial growth factor in Hep3B cells. *Biochemical Pharmacology, 61*(8), 947–954.

Daulatzai, M. A. (2017). Cerebral hypoperfusion and glucose hypometabolism: Key pathophysiological modulators promote neurodegeneration, cognitive impairment, and Alzheimer's disease. *Journal of Neuroscience Research, 95*(4), 943–972. https://doi.org/10.1002/jnr.23777.

Dore-Duffy, P., Owen, C., Balabanov, R., Murphy, S., Beaumont, T., & Rafols, J. A. (2000). Pericyte migration from the vascular wall in response to traumatic brain injury. *Microvascular Research, 60*(1), 55–69. https://doi.org/10.1006/mvre.2000.2244.

Drouin-Ouellet, J., Sawiak, S. J., Cisbani, G., Lagace, M., Kuan, W. L., Saint-Pierre, M., et al. (2015). Cerebrovascular and blood-brain barrier impairments in Huntington's disease: Potential implications for its pathophysiology. *Annals of Neurology, 78*(2), 160–177. https://doi.org/10.1002/ana.24406.

Elvidge, G. P., Glenny, L., Appelhoff, R. J., Ratcliffe, P. J., Ragoussis, J., & Gleadle, J. M. (2006). Concordant regulation of gene expression by hypoxia and 2-oxoglutarate-dependent dioxygenase inhibition: The role of HIF-1alpha, HIF-2alpha, and other pathways. *Journal of Biological Chemistry, 281*(22), 15215–15226. https://doi.org/10.1074/jbc.M511408200.

Engelhardt, S., Al-Ahmad, A. J., Gassmann, M., & Ogunshola, O. O. (2014a). Hypoxia selectively disrupts brain microvascular endothelial tight junction complexes through a hypoxia-inducible factor-1 (HIF-1) dependent mechanism. *Journal of Cellular Physiology, 229*(8), 1096–1105. https://doi.org/10.1002/jcp.24544.

Engelhardt, S., Huang, S. F., Patkar, S., Gassmann, M., & Ogunshola, O. O. (2015). Differential responses of blood-brain barrier associated cells to hypoxia and ischemia: A comparative study. *Fluids Barriers CNS, 12*, 4. https://doi.org/10.1186/2045-8118-12-4.

Engelhardt, S., Patkar, S., & Ogunshola, O. O. (2014b). Cell-specific blood-brain barrier regulation in health and disease: A focus on hypoxia. *British Journal of Pharmacology, 171*(5), 1210–1230. https://doi.org/10.1111/bph.12489.

Feng, S., Cen, J., Huang, Y., Shen, H., Yao, L., Wang, Y., et al. (2011). Matrix metalloproteinase-2 and – 9 secreted by leukemic cells increase the permeability of blood-brain barrier by disrupting tight junction proteins. *PLoS ONE, 6*(8), e20599. https://doi.org/10.1371/journal.pone.0020599.

Fernandez-Lopez, D., Faustino, J., Daneman, R., Zhou, L., Lee, S. Y., Derugin, N., et al. (2012). Blood-brain barrier permeability is increased after acute adult stroke but not neonatal stroke in the rat. *The Journal of Neuroscience, 32*(28), 9588–9600. https://doi.org/10.1523/JNEUROSCI.5977-11.2012.

Fischer, S., Clauss, M., Wiesnet, M., Renz, D., Schaper, W., & Karliczek, G. F. (1999). Hypoxia induces permeability in brain microvessel endothelial cells via VEGF and NO. *American Journal of Physiology, 276*(4 Pt 1), C812–C820.

Fischer, S., Wiesnet, M., Marti, H. H., Renz, D., & Schaper, W. (2004). Simultaneous activation of several second messengers in hypoxia-induced hyperpermeability of brain derived endothelial cells. *Journal of Cellular Physiology, 198*(3), 359–369. https://doi.org/10.1002/jcp.10417.

Fischer, S., Wobben, M., Marti, H. H., Renz, D., & Schaper, W. (2002). Hypoxia-induced hyperpermeability in brain microvessel endothelial cells involves VEGF-mediated changes in the expression of zonula occludens-1. *Microvascular Research, 63*(1), 70–80. https://doi.org/10.1006/mvre.2001.2367.

Freeze, W. M., Bacskai, B. J., Frosch, M. P., Jacobs, H. I. L., Backes, W. H., Greenberg, S. M., et al. (2019). Blood-Brain Barrier Leakage and Microvascular Lesions in Cerebral Amyloid Angiopathy. *Stroke, 50*(2), 328–335. https://doi.org/10.1161/STROKEAHA.118.023788.

Genetos, D. C., Cheung, W. K., Decaris, M. L., & Leach, J. K. (2010). Oxygen tension modulates neurite outgrowth in PC12 cells through a mechanism involving HIF and VEGF. *Journal of Molecular Neuroscience, 40*(3), 360–366. https://doi.org/10.1007/s12031-009-9326-0.

Ghiso, J., Fossati, S., & Rostagno, A. (2014). Amyloidosis associated with cerebral amyloid angiopathy: Cell signaling pathways elicited in cerebral endothelial cells. *Journal of Alzheimer's Disease, 42*(Suppl 3), 167–176. https://doi.org/10.3233/JAD-140027.

Greenberg, D. A., & Jin, K. (2013). Vascular endothelial growth factors (VEGFs) and stroke. *Cellular and Molecular Life Sciences, 70*(10), 1753–1761. https://doi.org/10.1007/s00018-013-1282-8.

Gussenhoven, R., Klein, L., Ophelders, D., Habets, D. H. J., Giebel, B., Kramer, B. W., et al. (2019). Annexin A1 as Neuroprotective Determinant for Blood-Brain Barrier Integrity in Neonatal Hypoxic-Ischemic Encephalopathy. *Clinical Medicine*, 8(2), https://doi.org/10.3390/jcm8020137.

Haarmann, A., Deiss, A., Prochaska, J., Foerch, C., Weksler, B., Romero, I., et al. (2010). Evaluation of soluble junctional adhesion molecule-A as a biomarker of human brain endothelial barrier breakdown. *PLoS ONE, 5*(10), e13568. https://doi.org/10.1371/journal.pone.0013568.

Hackett, P. H., & Roach, R. C. (2004). High altitude cerebral edema. *High Altitude Medicine & Biology, 5*(2), 136–146. https://doi.org/10.1089/1527029041352054.

Haley, M. J., & Lawrence, C. B. (2017). The blood-brain barrier after stroke: Structural studies and the role of transcytotic vesicles. *Journal of Cerebral Blood Flow & Metabolism, 37*(2), 456–470. https://doi.org/10.1177/0271678X16629976.

Helms, H. C., Abbott, N. J., Burek, M., Cecchelli, R., Couraud, P. O., Deli, M. A., et al. (2016). In vitro models of the blood-brain barrier: An overview of commonly used brain endothelial cell culture models and guidelines for their use. *Journal of Cerebral Blood Flow & Metabolism, 36*(5), 862–890. https://doi.org/10.1177/0271678X16630991.

Holloway, P. M., & Gavins, F. N. (2016). Modeling Ischemic Stroke In Vitro: Status Quo and Future Perspectives. *Stroke, 47*(2), 561–569. https://doi.org/10.1161/STROKEAHA.115.011932.

Jang, S., Zheng, C., Tsai, H. T., Fu, A. Z., Barac, A., Atkins, M. B., et al. (2016). Cardiovascular toxicity after antiangiogenic therapy in persons older than 65 years with advanced renal cell carcinoma. *Cancer, 122*(1), 124–130. https://doi.org/10.1002/cncr.29728.

Jin, K., Zhu, Y., Sun, Y., Mao, X. O., Xie, L., & Greenberg, D. A. (2002). Vascular endothelial growth factor (VEGF) stimulates neurogenesis in vitro and in vivo. *Proceedings of the National Academy of Sciences of the USA, 99*(18), 11946–11950. https://doi.org/10.1073/pnas.182296499.

Jin, X., Sun, Y., Xu, J., & Liu, W. (2015). Caveolin-1 mediates tissue plasminogen activator-induced MMP-9 up-regulation in cultured brain microvascular endothelial cells. *Journal of Neurochemistry, 132*(6), 724–730. https://doi.org/10.1111/jnc.13065.

Kanazawa, M., Igarashi, H., Kawamura, K., Takahashi, T., Kakita, A., Takahashi, H., et al. (2011). Inhibition of VEGF signaling pathway attenuates hemorrhage after tPA treatment. *Journal of Cerebral Blood Flow & Metabolism, 31*(6), 1461–1474. https://doi.org/10.1038/jcbfm.2011.9.

Kassner, A., & Merali, Z. (2015). Assessment of Blood-Brain Barrier Disruption in Stroke. *Stroke, 46*(11), 3310–3315. https://doi.org/10.1161/STROKEAHA.115.008861.

Ke, X. J., & Zhang, J. J. (2013). Changes in HIF-1alpha, VEGF, NGF and BDNF levels in cerebrospinal fluid and their relationship with cognitive impairment in patients with cerebral infarction. *Journal of Huazhong University of Science and Technology Medical Sciences, 33*(3), 433–437. https://doi.org/10.1007/s11596-013-1137-4.

Kilic, E., Kilic, U., Wang, Y., Bassetti, C. L., Marti, H. H., & Hermann, D. M. (2006). The phosphatidylinositol-3 kinase/Akt pathway mediates VEGF's neuroprotective activity and induces blood brain barrier permeability after focal cerebral ischemia. *FASEB Journal, 20*(8), 1185–1187. https://doi.org/10.1096/fj.05-4829fje.

Kim, E., Yang, J., Park, K. W., & Cho, S. (2018). Inhibition of VEGF Signaling Reduces Diabetes-Exacerbated Brain Swelling, but Not Infarct Size, in Large Cerebral Infarction in Mice. *Translational Stroke Research, 9*(5), 540–548. https://doi.org/10.1007/s12975-017-0601-z.

Kim, H., Lee, J. M., Park, J. S., Jo, S. A., Kim, Y. O., Kim, C. W., et al. (2008). Dexamethasone coordinately regulates angiopoietin-1 and VEGF: A mechanism of glucocorticoid-induced stabilization of blood-brain barrier. *Biochemical and Biophysical Research Communications, 372*(1), 243–248. https://doi.org/10.1016/j.bbrc.2008.05.025.

Kim, K. A., Shin, D., Kim, J. H., Shin, Y. J., Rajanikant, G. K., Majid, A., et al. (2018). Role of Autophagy in Endothelial Damage and Blood-Brain Barrier Disruption in Ischemic Stroke. *Stroke, 49*(6), 1571–1579. https://doi.org/10.1161/STROKEAHA.117.017287.

Kokubu, Y., Yamaguchi, T., & Kawabata, K. (2017). In vitro model of cerebral ischemia by using brain microvascular endothelial cells derived from human induced pluripotent stem cells. *Biochemical and Biophysical Research Communications, 486*(2), 577–583. https://doi.org/10.1016/j.bbrc.2017.03.092.

Koto, T., Takubo, K., Ishida, S., Shinoda, H., Inoue, M., Tsubota, K., et al. (2007). Hypoxia disrupts the barrier function of neural blood vessels through changes in the expression of claudin-5 in endothelial cells. *The American Journal of Pathology, 170*(4), 1389–1397. https://doi.org/10.2353/ajpath.2007.060693.

Kuntz, M., Mysiorek, C., Petrault, O., Petrault, M., Uzbekov, R., Bordet, R., et al. (2014). Stroke-induced brain parenchymal injury drives blood-brain barrier early leakage kinetics: A combined in vivo/in vitro study. *Journal of Cerebral Blood Flow & Metabolism, 34*(1), 95–107. https://doi.org/10.1038/jcbfm.2013.169.

Lafuente, J. V., Bermudez, G., Camargo-Arce, L., & Bulnes, S. (2016). Blood-Brain Barrier Changes in High Altitude. *CNS Neurological Disorders - Drug Targets, 15*(9), 1188–1197.

Lee, C. A. A., Seo, H. S., Armien, A. G., Bates, F. S., Tolar, J., & Azarin, S. M. (2018). Modeling and rescue of defective blood-brain barrier function of induced brain microvascular endothelial cells from childhood cerebral adrenoleukodystrophy patients. *Fluids Barriers CNS, 15*(1), 9. https://doi.org/10.1186/s12987-018-0094-5.

Lee, K., Lee, J. H., Boovanahalli, S. K., Jin, Y., Lee, M., Jin, X., et al. (2007). Aryloxyacetylamino)benzoic acid analogues: A new class of hypoxia-inducible factor-1 inhibitors. *Journal of Medicinal Chemistry, 50*(7), 1675–1684. https://doi.org/10.1021/jm0610292.

Lee, W. L. A., Michael-Titus, A. T., & Shah, D. K. (2017). Hypoxic-Ischaemic Encephalopathy and the Blood-Brain Barrier in Neonates. *Developmental Neuroscience, 39*(1–4), 49–58. https://doi.org/10.1159/000467392.

Lim, R. G., Quan, C., Reyes-Ortiz, A. M., Lutz, S. E., Kedaigle, A. J., Gipson, T. A., et al. (2017). Huntington's Disease iPSC-Derived Brain Microvascular Endothelial Cells Reveal WNT-Mediated Angiogenic and Blood-Brain Barrier Deficits. *Cell Reports, 19*(7), 1365–1377. https://doi.org/10.1016/j.celrep.2017.04.021.

Lin, L., Chen, H., Zhang, Y., Lin, W., Liu, Y., Li, T., et al. (2015). IL-10 Protects Neurites in Oxygen-Glucose-Deprived Cortical Neurons through the PI3K/Akt Pathway. *PLoS ONE, 10*(9), e0136959. https://doi.org/10.1371/journal.pone.0136959.

Lippmann, E. S., Al-Ahmad, A., Azarin, S. M., Palecek, S. P., & Shusta, E. V. (2014). A retinoic acid-enhanced, multicellular human blood-brain barrier model derived from stem cell sources. *Scientific Reports, 4*, 4160. https://doi.org/10.1038/srep04160.

Liu, J., Jin, X., Liu, K. J., & Liu, W. (2012). Matrix metalloproteinase-2-mediated occludin degradation and caveolin-1-mediated claudin-5 redistribution contribute to blood-brain barrier damage in early ischemic stroke stage. *The Journal of Neuroscience, 32*(9), 3044–3057. https://doi.org/10.1523/JNEUROSCI.6409-11.2012.

Liu, W., Hendren, J., Qin, X. J., Shen, J., & Liu, K. J. (2009). Normobaric hyperoxia attenuates early blood-brain barrier disruption by inhibiting MMP-9-mediated occludin degradation in focal cerebral ischemia. *Journal of Neurochemistry, 108*(3), 811–820. https://doi.org/10.1111/j.1471-4159.2008.05821.x.

Lochhead, J. J., McCaffrey, G., Quigley, C. E., Finch, J., DeMarco, K. M., Nametz, N., et al. (2010). Oxidative stress increases blood-brain barrier permeability and induces alterations in occludin during hypoxia-reoxygenation. *Journal of Cerebral Blood Flow & Metabolism, 30*(9), 1625–1636. https://doi.org/10.1038/jcbfm.2010.29.

Lopez-Iglesias, P., Alcaina, Y., Tapia, N., Sabour, D., Arauzo-Bravo, M. J., de la Maza, S., D., et al (2015). Hypoxia induces pluripotency in primordial germ cells by HIF1alpha stabilization and Oct4 deregulation. *Antioxid Redox Signal, 22*(3), 205–223. https://doi.org/10.1089/ars.2014.5871.

Lu, D., Mai, H. C., Liang, Y. B., Xu, B. D., Xu, A. D., & Zhang, Y. S. (2018). Beneficial Role of Rosuvastatin in Blood-Brain Barrier Damage Following Experimental Ischemic Stroke. *Frontiers in Pharmacology, 9*, 926. https://doi.org/10.3389/fphar.2018.00926.

Ma, Q., Dasgupta, C., Li, Y., Huang, L., & Zhang, L. (2017). MicroRNA-210 Suppresses Junction Proteins and Disrupts Blood-Brain Barrier Integrity in Neonatal Rat Hypoxic-Ischemic Brain Injury. International Journal of Molecular Sciences. 18(7), https://doi.org/10.3390/ijms18071356.

Mani, N., Khaibullina, A., Krum, J. M., & Rosenstein, J. M. (2005). Astrocyte growth effects of vascular endothelial growth factor (VEGF) application to perinatal neocortical explants: Receptor mediation and signal transduction pathways. *Experimental Neurology, 192*(2), 394–406. https://doi.org/10.1016/j.expneurol.2004.12.022.

Mani, N., Khaibullina, A., Krum, J. M., & Rosenstein, J. M. (2010). Vascular endothelial growth factor enhances migration of astroglial cells in subventricular zone neurosphere cultures. *Journal of Neuroscience Research, 88*(2), 248–257. https://doi.org/10.1002/jnr.22197.

Margaritescu, O., Pirici, D., & Margaritescu, C. (2011). VEGF expression in human brain tissue after acute ischemic stroke. *Romanian Journal of Morphology and Embryology, 52*(4), 1283–1292. doi:52041112831292 [pii].

Mark, K. S., & Davis, T. P. (2002). Cerebral microvascular changes in permeability and tight junctions induced by

hypoxia-reoxygenation. *American Journal of Physiology-Heart and Circulatory Physiology, 282*(4), H1485–H1494. https://doi.org/10.1152/ajpheart.00645.2001.

Martin-Aragon Baudel, M. A. S., Rae, M. T., Darlison, M. G., Poole, A. V., & Fraser, J. A. (2017). Preferential activation of HIF-2alpha adaptive signalling in neuronal-like cells in response to acute hypoxia. *PLoS ONE, 12*(10), e0185664. https://doi.org/10.1371/journal.pone.0185664.

Mathieu, J., Zhou, W., Xing, Y., Sperber, H., Ferreccio, A., Agoston, Z., et al. (2014). Hypoxia-inducible factors have distinct and stage-specific roles during reprogramming of human cells to pluripotency. *Cell Stem Cell, 14*(5), 592–605. https://doi.org/10.1016/j.stem.2014.02.012.

McCaffrey, G., Willis, C. L., Staatz, W. D., Nametz, N., Quigley, C. A., Hom, S., et al. (2009). Occludin oligomeric assemblies at tight junctions of the blood-brain barrier are altered by hypoxia and reoxygenation stress. *Journal of Neurochemistry, 110*(1), 58–71. https://doi.org/10.1111/j.1471-4159.2009.06113.x.

Medley, T. L., Furtado, M., Lam, N. T., Idrizi, R., Williams, D., Verma, P. J., et al. (2013). Effect of oxygen on cardiac differentiation in mouse iPS cells: Role of hypoxia inducible factor-1 and Wnt/beta-catenin signaling. *PLoS ONE, 8*(11), e80280. https://doi.org/10.1371/journal.pone.0080280.

Merali, Z., Huang, K., Mikulis, D., Silver, F., & Kassner, A. (2017). Evolution of blood-brain-barrier permeability after acute ischemic stroke. *PLoS ONE, 12*(2), e0171558. https://doi.org/10.1371/journal.pone.0171558.

Mimeault, M., & Batra, S. K. (2013). Hypoxia-inducing factors as master regulators of stemness properties and altered metabolism of cancer- and metastasis-initiating cells. *Journal of Cellular and Molecular Medicine, 17*(1), 30–54. https://doi.org/10.1111/jcmm.12004.

Mo, S. J., Hong, J., Chen, X., Han, F., Ni, Y., Zheng, Y., et al. (2016). VEGF-mediated NF-kappaB activation protects PC12 cells from damage induced by hypoxia. *Neuroscience Letters, 610*, 54–59. https://doi.org/10.1016/j.neulet.2015.10.051.

Na, J. I., Na, J. Y., Choi, W. Y., Lee, M. C., Park, M. S., Choi, K. H., et al. (2015). The HIF-1 inhibitor YC-1 decreases reactive astrocyte formation in a rodent ischemia model. *American Journal of Translational Research, 7*(4), 751–760.

Naik, P., & Cucullo, L. (2012). In vitro blood-brain barrier models: Current and perspective technologies. *Journal of Pharmaceutical Sciences, 101*(4), 1337–1354. https://doi.org/10.1002/jps.23022.

Nakashima, Y., Miyagi-Shiohira, C., Noguchi, H., & Omasa, T. (2018). Atorvastatin Inhibits the HIF1alpha-PPAR Axis, Which Is Essential for Maintaining the Function of Human Induced Pluripotent Stem Cells. *Molecular Therapy, 26*(7), 1715–1734. https://doi.org/10.1016/j.ymthe.2018.06.005.

Natah, S. S., Srinivasan, S., Pittman, Q., Zhao, Z., & Dunn, J. F. (2009). Effects of acute hypoxia and hyperthermia on the permeability of the blood-brain barrier in adult rats. *Journal of Applied Physiology (1985), 107*(4), 1348–1356. https://doi.org/10.1152/japplphysiol.91484.2008.

Nation, D. A., Sweeney, M. D., Montagne, A., Sagare, A. P., D'Orazio, L. M., Pachicano, M., et al. (2019). Blood-brain barrier breakdown is an early biomarker of human cognitive dysfunction. *Nature Medicine*. https://doi.org/10.1038/s41591-018-0297-y.

Neuwelt, E. A., Bauer, B., Fahlke, C., Fricker, G., Iadecola, C., Janigro, D., et al. (2011). Engaging neuroscience to advance translational research in brain barrier biology. *Nature Reviews Neuroscience, 12*(3), 169–182. https://doi.org/10.1038/nrn2995.

Nobes, C. D., Hay, W. W. Jr., & Brand, M. D. (1990). The mechanism of stimulation of respiration by fatty acids in isolated hepatocytes. *Journal of Biological Chemistry, 265*(22), 12910–12915.

O'Donnell, M. E. (2014). Blood-brain barrier Na transporters in ischemic stroke. *Advances in Pharmacology, 71*, 113–146. https://doi.org/10.1016/bs.apha.2014.06.011.

Ogunshola, O. O. (2011). In vitro modeling of the blood-brain barrier: Simplicity versus complexity. *Current Pharmaceutical Design, 17*(26), 2755–2761. doi:BSP/CPD/E-Pub/000559 [pii].

Ogunshola, O. O., & Al-Ahmad, A. (2012). HIF-1 at the blood-brain barrier: A mediator of permeability? *High Altitude Medicine & Biology, 13*(3), 153–161. https://doi.org/10.1089/ham.2012.1052.

Ohab, J. J., Fleming, S., Blesch, A., & Carmichael, S. T. (2006). A neurovascular niche for neurogenesis after stroke. *The Journal of Neuroscience, 26*(50), 13007–13016. https://doi.org/10.1523/JNEUROSCI.4323-06.2006.

Orchard, P. J., Nascene, D. R., Miller, W. P., Gupta, A., Kenney-Jung, D., & Lund, T. C. (2019). Successful donor engraftment and repair of the blood brain barrier in cerebral adrenoleukodystrophy. *Blood*. https://doi.org/10.1182/blood-2018-11-887240.

Page, S., Munsell, A., & Al-Ahmad, A. J. (2016). Cerebral hypoxia/ischemia selectively disrupts tight junctions complexes in stem cell-derived human brain microvascular endothelial cells. *Fluids Barriers CNS, 13*(1), 16. https://doi.org/10.1186/s12987-016-0042-1.

Palmiotti, C. A., Prasad, S., Naik, P., Abul, K. M., Sajja, R. K., Achyuta, A. H., et al. (2014). In vitro cerebrovascular modeling in the 21st century: Current and prospective technologies. *Pharmaceutical Research, 31*(12), 3229–3250. https://doi.org/10.1007/s11095-014-1464-6.

Patel, R., Page, S., & Al-Ahmad, A. J. (2017). Isogenic blood-brain barrier models based on patient-derived stem cells display inter-individual differences in cell maturation and functionality. *Journal of Neurochemistry, 142*(1), 74–88. https://doi.org/10.1111/jnc.14040.

Perriere, N., Demeuse, P., Garcia, E., Regina, A., Debray, M., Andreux, J. P., et al. (2005). Puromycin-based purification of rat brain capillary endothelial cell cultures. Effect on the expression of blood-brain barrier-specific properties. *Journal of Neurochemistry, 93*(2), 279–289. https://doi.org/10.1111/j.1471-4159.2004.03020.x.

Pikula, A., Beiser, A. S., Chen, T. C., Preis, S. R., Vorgias, D., DeCarli, C., et al. (2013). Serum brain-derived neurotrophic factor and vascular endothelial growth factor levels are associated with risk of stroke and vascular brain injury: Framingham Study. *Stroke, 44*(10), 2768–2775. https://doi.org/10.1161/STROKEAHA.113.001447.

Plaschke, K., Staub, J., Ernst, E., & Marti, H. H. (2008). VEGF overexpression improves mice cognitive abilities after unilateral common carotid artery occlusion. *Experimental Neurology, 214*(2), 285–292. https://doi.org/10.1016/j.expneurol.2008.08.014.

Prakash, R., & Carmichael, S. T. (2015). Blood-brain barrier breakdown and neovascularization processes after stroke and traumatic brain injury. *Current Opinion in Neurology, 28*(6), 556–564. https://doi.org/10.1097/WCO.0000000000000248.

Roskoski, R. Jr. (2017). Vascular endothelial growth factor (VEGF) and VEGF receptor inhibitors in the treatment of renal cell carcinomas. *Pharmacological Research, 120*, 116–132. https://doi.org/10.1016/j.phrs.2017.03.010.

Ruan, L., Wang, B., ZhuGe, Q., & Jin, K. (2015). Coupling of neurogenesis and angiogenesis after ischemic stroke. *Brain Research, 1623*, 166–173. https://doi.org/10.1016/j.brainres.2015.02.042.

Sajja, R. K., Prasad, S., & Cucullo, L. (2014). Impact of altered glycaemia on blood-brain barrier endothelium: An in vitro study using the hCMEC/D3 cell line. *Fluids Barriers CNS, 11*(1), 8. https://doi.org/10.1186/2045-8118-11-8.

Schmid-Brunclik, N., Burgi-Taboada, C., Antoniou, X., Gassmann, M., & Ogunshola, O. O. (2008). Astrocyte responses to injury: VEGF simultaneously modulates cell death and proliferation.

American Journal of Physiology-Regulatory, Integrative and Comparative Physiology, 295(3), R864–R873. https://doi.org/10.1152/ajpregu.00536.2007.

Schoch, H. J., Fischer, S., & Marti, H. H. (2002). Hypoxia-induced vascular endothelial growth factor expression causes vascular leakage in the brain. *Brain, 125*(Pt 11), 2549–2557.

Suzuki, Y., Nagai, N., & Umemura, K. (2016). A Review of the Mechanisms of Blood-Brain Barrier Permeability by Tissue-Type Plasminogen Activator Treatment for Cerebral Ischemia. *Frontiers in Cellular Neuroscience, 10*, 2. https://doi.org/10.3389/fncel.2016.00002.

Sweeney, M. D., Montagne, A., Sagare, A. P., Nation, D. A., Schneider, L. S., Chui, H. C., et al. (2019). Vascular dysfunction-The disregarded partner of Alzheimer's disease. *Alzheimers Dementia, 15*(1), 158–167. https://doi.org/10.1016/j.jalz.2018.07.222.

Turner, R. J., & Sharp, F. R. (2016). Implications of MMP9 for Blood Brain Barrier Disruption and Hemorrhagic Transformation Following Ischemic Stroke. *Frontiers in Cellular Neuroscience, 10*, 56. https://doi.org/10.3389/fncel.2016.00056.

Vatine, G. D., Al-Ahmad, A., Barriga, B. K., Svendsen, S., Salim, A., Garcia, L., et al. (2017). Modeling Psychomotor Retardation using iPSCs from MCT8-Deficient Patients Indicates a Prominent Role for the Blood-Brain Barrier. *Cell Stem Cell, 20*(6), 831–843 e835. https://doi.org/10.1016/j.stem.2017.04.002.

Vogel, C., Bauer, A., Wiesnet, M., Preissner, K. T., Schaper, W., Marti, H. H., et al. (2007). Flt-1, but not Flk-1 mediates hyperpermeability through activation of the PI3-K/Akt pathway. *Journal of Cellular Physiology, 212*(1), 236–243. https://doi.org/10.1002/jcp.21022.

Wang, Q., Yang, L., & Wang, Y. (2015). Enhanced differentiation of neural stem cells to neurons and promotion of neurite outgrowth by oxygen-glucose deprivation. *International Journal of Developmental Neuroscience, 43*, 50–57. https://doi.org/10.1016/j.ijdevneu.2015.04.009.

Wang, R., Zhang, X., Zhang, J., Fan, Y., Shen, Y., Hu, W., et al. (2012). Oxygen-glucose deprivation induced glial scar-like change in astrocytes. *PLoS ONE, 7*(5), e37574. https://doi.org/10.1371/journal.pone.0037574.

Wang, Y., Jin, K., Mao, X. O., Xie, L., Banwait, S., Marti, H. H., et al. (2007). VEGF-overexpressing transgenic mice show enhanced post-ischemic neurogenesis and neuromigration. *Journal of Neuroscience Research, 85*(4), 740–747. https://doi.org/10.1002/jnr.21169.

Wang, Y., Sang, A., Zhu, M., Zhang, G., Guan, H., Ji, M., et al. (2016). Tissue factor induces VEGF expression via activation of the Wnt/beta-catenin signaling pathway in ARPE-19 cells. *Molecular Vision, 22*, 886–897.

Wang, Z. G., Cheng, Y., Yu, X. C., Ye, L. B., Xia, Q. H., Johnson, N. R., et al. (2016). bFGF Protects Against Blood-Brain Barrier Damage Through Junction Protein Regulation via PI3K-Akt-Rac1 Pathway Following Traumatic Brain Injury. *Molecular Neurobiology, 53*(10), 7298–7311. https://doi.org/10.1007/s12035-015-9583-6.

Weksler, B. B., Subileau, E. A., Perriere, N., Charneau, P., Holloway, K., Leveque, M., et al. (2005). Blood-brain barrier-specific properties of a human adult brain endothelial cell line. *FASEB Journal, 19*(13), 1872–1874. https://doi.org/10.1096/fj.04-3458fje.

Witt, K. A., Mark, K. S., Hom, S., & Davis, T. P. (2003). Effects of hypoxia-reoxygenation on rat blood-brain barrier permeability and tight junctional protein expression. *American Journal of Physiology-Heart and Circulatory Physiology, 285*(6), H2820–H2831. https://doi.org/10.1152/ajpheart.00589.2003.

Wu, C., Chen, J., Chen, C., Wang, W., Wen, L., Gao, K., et al. (2015). Wnt/beta-catenin coupled with HIF-1alpha/VEGF signaling pathways involved in galangin neurovascular unit protection from focal cerebral ischemia. *Scientific Reports, 5*, 16151. https://doi.org/10.1038/srep16151.

Wu, F., Chen, Z., Tang, C., Zhang, J., Cheng, L., Zuo, H., et al. (2017). Acid fibroblast growth factor preserves blood-brain barrier integrity by activating the PI3K-Akt-Rac1 pathway and inhibiting RhoA following traumatic brain injury. *American Journal of Translational Research, 9*(3), 910–925.

Yan, J., Zhang, Z., & Shi, H. (2012). HIF-1 is involved in high glucose-induced paracellular permeability of brain endothelial cells. *Cellular and Molecular Life Sciences, 69*(1), 115–128. https://doi.org/10.1007/s00018-011-0731-5.

Yan, J., Zhou, B., Taheri, S., & Shi, H. (2011). Differential effects of HIF-1 inhibition by YC-1 on the overall outcome and blood-brain barrier damage in a rat model of ischemic stroke. *PLoS ONE, 6*(11), e27798. https://doi.org/10.1371/journal.pone.0027798.

Yang, T., Roder, K. E., & Abbruscato, T. J. (2007). Evaluation of bEnd5 cell line as an in vitro model for the blood-brain barrier under normal and hypoxic/aglycemic conditions. *Journal of Pharmaceutical Sciences, 96*(12), 3196–3213. https://doi.org/10.1002/jps.21002.

Yang, Y., & Rosenberg, G. A. (2011). Blood-brain barrier breakdown in acute and chronic cerebrovascular disease. *Stroke, 42*(11), 3323–3328. https://doi.org/10.1161/STROKEAHA.110.608257.

Yang, Y., Thompson, J. F., Taheri, S., Salayandia, V. M., McAvoy, T. A., Hill, J. W., et al. (2013). Early inhibition of MMP activity in ischemic rat brain promotes expression of tight junction proteins and angiogenesis during recovery. *Journal of Cerebral Blood Flow & Metabolism, 33*(7), 1104–1114. https://doi.org/10.1038/jcbfm.2013.56.

Yeh, W. L., Lu, D. Y., Lin, C. J., Liou, H. C., & Fu, W. M. (2007). Inhibition of hypoxia-induced increase of blood-brain barrier permeability by YC-1 through the antagonism of HIF-1alpha accumulation and VEGF expression. *Molecular Pharmacology, 72*(2), 440–449. https://doi.org/10.1124/mol.107.036418.

Yu, J., Vodyanik, M. A., Smuga-Otto, K., Antosiewicz-Bourget, J., Frane, J. L., Tian, S., et al. (2007). Induced pluripotent stem cell lines derived from human somatic cells. *Science, 318*(5858), 1917–1920. https://doi.org/10.1126/science.1151526.

Zhang, Q. L., Cui, B. R., Li, H. Y., Li, P., Hong, L., Liu, L. P., et al. (2013). MAPK and PI3K pathways regulate hypoxia-induced atrial natriuretic peptide secretion by controlling HIF-1 alpha expression in beating rabbit atria. *Biochemical and Biophysical Research Communications, 438*(3), 507–512. https://doi.org/10.1016/j.bbrc.2013.07.106.

Zhang, S., An, Q., Wang, T., Gao, S., & Zhou, G. (2018). Autophagy- and MMP-2/9-mediated Reduction and Redistribution of ZO-1 Contribute to Hyperglycemia-increased Blood-Brain Barrier Permeability During Early Reperfusion in Stroke. *Neuroscience, 377*, 126–137. https://doi.org/10.1016/j.neuroscience.2018.02.035.

Zhang, Z., Yan, J., & Shi, H. (2016). Role of Hypoxia Inducible Factor 1 in Hyperglycemia-Exacerbated Blood-Brain Barrier Disruption in Ischemic Stroke. *Neurobiology of Disease, 95*, 82–92. https://doi.org/10.1016/j.nbd.2016.07.012.

Zhang, Z. G., Zhang, L., Jiang, Q., Zhang, R., Davies, K., Powers, C., et al. (2000). VEGF enhances angiogenesis and promotes blood-brain barrier leakage in the ischemic brain. *Journal of Clinical Investigation, 106*(7), 829–838. https://doi.org/10.1172/JCI9369.

Zhong, J., Chan, A., Morad, L., Kornblum, H. I., Fan, G., & Carmichael, S. T. (2010). Hydrogel matrix to support stem cell survival after brain transplantation in stroke.

Neurorehabilitation and Neural Repair, 24(7), 636–644. https://doi.org/10.1177/1545968310361958.

Zhu, H., Wang, Z., Xing, Y., Gao, Y., Ma, T., Lou, L., et al. (2012). Baicalin reduces the permeability of the blood-brain barrier during hypoxia in vitro by increasing the expression of tight junction proteins in brain microvascular endothelial cells. *Journal of Ethnopharmacology, 141*(2), 714–720. https://doi.org/10.1016/j.jep.2011.08.063.